1	Identification of phenological QTLs using a combination of
2	High and Low-Coverage Whole Genome Sequencing in
3	Japanese plum (Prunus salicina Lindl.)
4 5 6	María Nicolás-Almansa ^{a,b} , David Ruiz ^a , Alfonso Guevara ^c , Manuel Rubio ^a , Pedro Martínez-Gómez ^a , Pat J Brown ^d , Pedro J Martínez-García ^{a,*}
7	
8 9	^a Department of Plant Breeding, CEBAS-CSIC, PO Box 164, E-30100 Espinardo, Murcia, Spain.
10 11 12 13	^b Present address: Department of Applied Biology, Escuela Politécnica Superior de Orihuela, University Miguel Hernández, Ctra. Beniel km. 3.2, Orihuela, 03312 Alicante, Spain
14 15	^c Department of Hortofruticulture, IMIDA, Murcia, Spain
16	d Department of Plant Sciences, University of California, Davis, CA 95616, USA.
17 18	* Corresponding author
19	E-mail address: pjmgarcia@cebas.csic.es
20 21 22	
23	
24	
25	
2627	
28	
29	
30	
31	<i>Y</i> ***
32	
33	
34	
35	
36 37 38	© The Author(s) 2025. Published by Oxford University Press. This is an Open Access article distributed under the terms of the Creative Commons Attribution License https://creativecommons.org/licenses/by/4.0/, which permits

unrestricted reuse, distribution, and reproduction in any medium, provided the

39

40

original work is properly cited.

Abstract

41

42

43

44

45 46

47 48

49

50

51

52 53

54

55

56

57

58

59

60

61

62 63 The genetic control of phenological traits in Japanese plum (Prunus salicina Lindl.) was investigated through quantitative trait loci (QTL) analysis in three segregating F₁ populations: 'Black Splendor' × 'Pioneer' (BS×PIO), 'Red Beaut' × 'Black Splendor' (RB×BS), and 'Red Beaut' × 'Santa Rosa Precoz' (RB×SRP), comprising 121, 103, and 103 seedlings, respectively. Whole-genome sequencing (~80x) was conducted for the four parents, and progenies were genotyped using a cost-efficient reduced-representation sequencing strategy. SNPs heterozygous in one parent and homozygous in the other were used to build six parental linkage maps. Phenological traits—including beginning, full, and end of flowering (BF, FF, EF), flowering intensity (FI), ripening date (RD), fruit development period (FDP), and productivity (P)—were evaluated over three years. A total of 53 QTLs were identified for flowering stages, 16 for RD, 18 for FDP, 10 for FI, and 16 for P. Many QTLs were stable across years. Major QTLs for flowering traits were mapped to LG1, LG2, LG4, and LG6, with a strong QTL for FF on LG6 of 'Black Splendor'. In BS×PIO, BF was uncorrelated with FF and EF, indicating distinct genetic control likely inherited from 'Pioneer', a low-chill cultivar. RD and FDP were consistently associated with LG4, while productivity QTLs were detected on LG1, LG2, and LG4, often overlapping, suggesting pleiotropic or tightly linked loci. In addition, candidate genes within stable QTLs were detected, providing immediate targets for functional studies. This study provides one of the first genome-wide QTL analyses of phenology in Japanese plum using low-coverage WGS (lcWGS) and offers valuable tools for markerassisted breeding in this species.

64 65

Keywords: Phenology - Prunus salicina -- QTL - breeding - lcWGS

1. Introduction

The *Prunus* genus encompasses economically significant species in global agriculture, including *P. persica* (peach), *P. avium* (sweet cherry), *P. dulcis* (almond), *P. armeniaca* (apricot) and plum species. The plum species, Japanese plum (*Prunus salicina* Lindl.) and European plum (*P. domestica* L.), rank as the second most important stone fruit crop following peaches, with a worldwide production of around 12 million tons [1]. Unlike the hexaploid European plum (6n = 2x = 48), the Japanese plum has a diploid genome (2n = 2x = 16). It originated in China, but its modern breeding history began in California by Luther Burbank, who introduced interspecific crosses with several diploid plums, such as *P. americana* Marshall, *P. hortulana* L. H. Bailey, *P. munsoniana* W. Wight & Hedrick, or *P. simonii* Carrière, to enhance its adaptation to local environments. Consequently, the term "Japanese plum" refers to a diverse group of hybrids derived from crosses involving up to 15 different *Prunus* species rather than a single pure species [2].

Similar to other *Prunus* species and woody crops, plums typically have long breeding cycles due to extended juvenile periods, complex reproductive biology, and a high degree of heterozygosity [3]. The development of new cultivars is particularly needed in plums, as global production largely depends on a limited number of heirloom cultivars [4]. The improved cultivars can compensate for the shortcomings of these heirloom cultivars. While the most advanced plum breeding programs are primarily based in California [2], significant efforts are also underway in countries such as China, Japan, Chile, and Spain [5,6]. The improvement of phenological traits, such as flowering time or ripening date, remains one of the main breeding objectives [2,7], but these traits are also increasingly affected by climate change [8,9]. In regions such as Badajoz, Spain, reduced winter chill threatens dormancy release and flowering stability [10,11].

The use of biotechnological approaches, such as marker-assisted selection (MAS) or genomics, can help accelerate the highly time-consuming breeding process in plum to develop climate-resilient cultivars. The availability of molecular markers in Japanese plum remains limited, with initial efforts focused primarily on self-incompatibility markers, which support the evaluation of intercompatibility among genotypes and aid in crossbreeding strategies [12]. More recently, markers associated with skin colour [13] and flesh colour [14] have been developed, enabling precise prediction of red pigmentation in both tissues.

Compared to other *Prunus* species, only a few studies have focused on the identification of quantitative trait loci (QTLs) linked to phenological and fruit quality traits in Japanese plum [15,16]. These studies have identified QTLs for traits such as flowering time, ripening date, and flavonoid content, primarily using linkage mapping based on genotyping-by-sequencing (GBS). The main drawback of these studies is that they relied on the peach genome [17] as a reference for read mapping, relying on the high synteny between *Prunus* species [18].

More recently, the release of a new reference genome for *P. salicina* has allowed the improvement of these previous results [19]. These authors employed the genome of cv. 'Sanyueli' [20] to improve previous linkage maps and to elucidate QTLs associated with phenolic compound content, specifically flavan-3-ols. Although, GBS is a relatively inexpensive method for genotyping large numbers of samples and provides more SNPs than SNP arrays [21], new

117 applications, also based on the reduced representation of the genome, have been 118 developed in the last ten years, which greatly reduce the cost of sequencing [22]. 119 Another cost-effective solution for F₁ populations typically used in fruit tree 120 breeding was recently proposed [23]. These authors suggested that the use of the Smooth Descent (SD) algorithm, with long-read sequencing of the parents 121 and low-depth sequencing with short reads of the descendants would reduce 122 genotyping costs. However, the application of these new approaches is clearly 123 124 scarce in Japanese plum and in *Prunus* species in general.

The main goal of this study was to investigate the genetic control of key phenological traits in Japanese plum through QTL analysis of three F₁ populations. We aimed to construct linkage maps and identify stable QTLs and candidate genes using an integrated whole-genome sequencing strategy.

129130

153

154

155

156157

158

125

126 127

128

2. Materials and Methods

131 2.1. Plant material

- The plant material assayed included three F₁ progenies from intraspecific crosses 132 133 of four Japanese plum cultivars: 'Black Splendor' x 'Pioneer' (BSxPIO); 'Red Beaut' x 'Black Splendor' (RBxBS) and 'Red Beaut' x 'Santa Rosa Precoz' 134 135 (RB×SRP) with 121, 103 and 103 seedlings, respectively (Fig. 1). All parental 136 trees were grafted onto the commercial rootstock Mariana 2624, whereas the 137 progenies were grown on their own root. Pedigrees of the parental genotypes are shown in Fig. 2, and their main agronomic traits are summarized in Table S1. The 138 139 crosses followed the standard methodology of a classical breeding program, 140 including controlled pollination under mesh in the field, embryo rescue, 141 greenhouse acclimation, and subsequent field plantation. Crosses were performed as part of the Japanese plum breeding program developed jointly by 142 143 CEBAS-CSIC and IMIDA of Murcia (Spain). The RBxBS and RBxSRP seedlings 144 were planted on field conditions in 2013, while BSxPIO progeny was planted two 145 years later. All seedlings were cultivated in the same experimental orchard 146 located in Calasparra (Murcia, southeastern Spain; lat. 38°16'N, long. 1°35'W; 147 350 m altitude) according to standard Japanese plum orchard management.
- 148 2.2. DNA extraction
- Young leaves were sampled during the spring season and preserved at -80 °C until DNA extraction. The DNA isolation process was conducted following a modified version of the CTAB method initially outlined by [26]. The DNA concentration was precisely quantified by Qubit 2.0.
 - 2.3. Whole Genome Sequencing (WGS) and assembly of parental genomes

Parental genomes were sequenced at ~80x coverage by Novogene using Illumina paired-end technology. Libraries were prepared via fragmentation, adapter ligation, PCR amplification, and quality-checked using a Bioanalyzer and qPCR. De novo assembly was performed with MaSuRCA [27], and assembly quality was evaluated with QUAST [28]. Read alignment back to the assemblies

was done using Bowtie2 [29], and genome completeness was assessed using BUSCO v5 with the embryophyta_odb10 dataset [30].

Variant calling was performed by aligning trimmed reads to the *Prunus salicina* cv. Sanyueli v2.0. genome using BWA-MEM [31]. SAM files were converted to BAM, sorted, and indexed with SAMtools [32] and Picard tools [33]. Variants were called using BCFtools v1.1356 [32] and filtered with the following thresholds: QUAL > 19 && DP > 2\$ && (AC/AN) > 0.05 && MQ > 20.

2.4 Calling SNPs on progeny from reduced-representation Illumina data

Genotyping-by-sequencing (GBS) libraries were prepared in 96-well plates using simultaneous restriction-ligation with either HindIII-HF or PstI-HF in combination with Msel and T4 DNA Ligase (New England Biolabs, Frankfurt) [34]. Individual barcoded libraries were pooled by 96-well plate, cleaned using Ampure XP beads, PCR amplified, and then cleaned again with Ampure XP beads before loading onto an Agilent Bioanalyzer 2100 in a DNA7500 chip. Libraries were adjusted to 10 nmol before submission to the UC Davis Genome Center for SR100 sequencing on a HiSeq4000 instrument. All the data were in a single Illumina HiSeq lane. The TASSEL GBS pipeline [35] and BWA [31] were used to align 64 bp tags to the *Prunus salicina* cv. 'Sanyueli' assembly [20], retaining only tags with a BWA MAPQ score of at least 20. Subsequently, SNPs were filtered separately for each parent in each population using the corresponding genome assembly. Only assembly SNPs supported with a depth of at least 8X in both parents were considered, and only SNPs beterozygous in the focal parent and homozygous in the other parent were included in the filtered SNP list for each parent of each population. The filtered SNP lists (eight in total) were used as input for FSFHap (Full-Sib Family Haplotype Imputation) [36] to correct for undercalling of heterozygous genotypes, and FSFHap output was used for linkage map construction.

2.5. Evaluation of phenological traits and data analysis

The phenological traits of interest, including the beginning of flowering (BF), full flowering (FF), end of flowering (EF), flowering intensity (FI), ripening date (RD), fruit development period (FDP) and productivity (P), were evaluated for three consecutive years (2019, 2020 and 2021) in the offspring and their respective parents. The assessment of flowering time was conducted periodically in the orchard at 3-4 day intervals, with results expressed in Julian days. BF was determined when 5% of the flowers had opened, FF was recorded at stage 65 according to the BBCH scale [37] when 50% of the flowers had opened, and EF was recorded when 90% of the flowers had opened. FI was quantified on a scale from 0 to 3. Additionally, RD was determined at physiological maturity, characterized by appropriate fruit firmness and color, while P was visually scored on a scale from 0 (null) to 5 (maximum). Finally, FDP was calculated as the number of days between FF and RD.

Statistical analyses were performed using IBM SPSS (Version 27) [38]. Frequency histograms were generated to show the distribution of seedlings for each trait, year, and population. The normality of all phenotypic datasets was tested using the Kolmogorov-Smirnov test with Lilliefors correction, considering

206 genotype and year as independent factors. Traits that did not meet the normality criteria were analyzed using the non-parametric Kruskal-Wallis test. Additionally, 207 208 Spearman correlation coefficients were calculated to assess the relationships 209 between traits within the same year and the interannual correlations for each trait, 210 using raw data and a significance level of $p \le 0.05$ for the three populations. 211 Principal components analysis (PCA) was performed on the phenological data to 212 facilitate visualization of the complete dataset in a reduced-dimensional plot, thereby identifying related groups, trends, or outliers. Spearman correlations, 213 214 PCA calculations, and plotting were carried out using the R packages 'corrplot' 215 [39], 'factoextra' [40], and 'FactoMineR' [41].

216217

218219

220

221

222223

224

225

226227

228

229230

231

232

2.6. Linkage Map Construction and Quantitative Trait Loci Analysis Genetic linkage maps were constructed for each parent in the BS×PIO. RB×BS. and RB×SRP populations using JoinMap® 4.1 [42]. SNP markers heterozygous in one parent and homozygous in the other (<|mx||> or <nnxnp>) were used. Markers with >40% missing data, significant segregation distortion (χ^2 , p < 0.001), or complete redundancy (Similarity of Loci = 1) were excluded. Mapping employed the Maximum Likelihood algorithm with Haldane's function, a recombination frequency threshold of 0.4, and LOD scores between 6-10. SNP positions were based on the Prunus salicina 'Sanyueli' v2.0 genome [16]. Six parental maps were generated independently, with no consensus map constructed. QTL analysis was performed in MapQTL® 6 [43] using the Kruskal-Wallis non-parametric test and 1000 permutations to define trait-specific significance thresholds (α < 0.05, 0.01, 0.001). Stable QTLs were defined as those consistently detected with p < 0.05 across all three years. The most significant markers within these QTLs were further analyzed for genotypephenotype associations, assessed by Kruskal-Wallis tests and visualized with the R packages 'LinkageMapView' [44] and 'ggplot2' [45].

233234

235

236

237

238239

240

241

244

245

246247

248249

250

251

3. Results

3.1. Genome Sequencing and assembly

The total number of raw reads was 720,391,200, with the highest number obtained for 'Santa Rosa Precoz' (193,383,502) and the lowest for 'Black Splendor' (174,744,788). The total data output from the sequencer was 108.1 Gb. After trimming the raw reads, more than 89% of the raw data were retained. The highest number of retained reads was observed for BS, with 90.03% (157,321,936) (Table S2).

242 (157,321,936) (Table S2)243 The lengths of the a

The lengths of the assembled genomes ranged from 256.42 Mb for SRP to 239.11 Mb for BS. Overall, a relatively small N50 value was observed for all genomes, with BS exhibiting the highest N50, indicating a higher proportion of longer contigs. The GC content was consistent across all genomes, averaging approximately 37%. The SRP genome had the highest number of contigs (97,639), reflecting greater fragmentation, while the BS genome contained the fewest (81,968). However, BS also had the largest contig, suggesting better representation of long continuous sequences. Furthermore, BS exhibited a greater total length of long contigs (≥ 10,000 bp and ≥ 25,000 bp), indicating that

despite having fewer contigs, they are substantially longer. All assemblies showed zero ambiguous sequences, indicating a high level of precision in the genome assembly process (Table S3).

After quality control, reads were realigned to the genome assemblies to assess similarity. All reads from the four parental assemblies were paired, with SRP showing the highest number of paired reads (96.7 million), followed by PIO (88.5 million), RB (87.6 million), and BS (87.4 million). The assemblies exhibited high alignment quality, with approximately 50% of reads aligning consistently at the correct distance and orientation to the MaSuRCA assemblies. Notably, the PIO and BS assemblies had the highest exact alignment rates (PIO: 51.61%; BS: 52.06%) and the highest overall alignment rate (94.34%) (Table S4).

The BUSCO analysis, based on the set of single-copy orthologs, showed that more than 80% of the expected genes were identified as complete (81.9% in SRP, 84.5% in PIO, 83.6% in RB, and 84.9% in BS) for the MASURCA assembly (Table S5).

3.2. Genetic Variation Analysis in the Parental Genotypes

252253

254

255

256

257258

259

260

261

262

263264

265266

267268

269

270

271

272

273

274

275

276

277

278279

280

281

282

283

284

285 286

287

288 289

290

291

292293

294

295

Regarding small genetic variation, a total of 9,223,636 genetic variants were identified using the analytical pipeline employed in this study. This dataset included 276,491 deletions, 284,641 small insertions, and 8,662,504 SNPs (Table S6). To refine the dataset, SNPs with two or more alternative alleles in the VCF file were excluded, resulting in a final set of 8,616,483 SNPs. This filtered set was subsequently used to calculate the number of transitions and transversions. Within this final SNP dataset, 59% were transitions (5,067,800 and 41% were transversions (3,548,683 loci). transition/transversion (Ts/Tv) ratio of 1.44 for SRP, 1.43 for PIO, 1.43 for RB, and 1.41 for BS. Among the transition variants, A/G and C/T substitutions were the most frequent and occurred at similar rates. Among transversions, A/T substitutions exhibited the highest frequency (~32%), whereas C/G substitutions were the least frequent (~16%) (Table S7).

3.3. Genotypic characterization of the offspring

Two independent reduced representation libraries were prepared for each DNA sample using two different restriction enzymes, HindIII and Pstl. The average number of barcoded reads per sample was similar between both restriction enzymes, with a mean of 339,194 for HindIII and 329,254 for Pstl. Likewise, the proportion of barcoded reads that successfully aligned to the plum reference genome was comparable, reaching 87.4% for HindIII and 89.5% for Pstl.

Of the 384 DNA samples analyzed, 11 (2.9%) had fewer than 10,000 reads in both libraries, indicating low DNA quality. Additionally, seven samples (1.8%) had fewer than 10,000 reads only in the PstI library, whereas 24 samples (6.3%) had fewer than 10,000 reads exclusively in the HindIII library. These findings suggest that the PstI library preparation protocol may be slightly more robust than

HindIII. The number of raw SNPs identified per haplotype of each population was at least twice as high in the HindIII library compared to the PstI library (Table S8).

SNPs from both libraries were pooled and depth-filtered (genotypes with depth less than 5 were set to missing) before imputation with FSFHap. This process led to the loss of a substantial number of low-coverage SNPs. Of the 48 chromosomes targeted for imputation (8 plum chromosomes × 3 populations × 2 parents), two failed: chromosome 8 of 'Black Splendor' could not be imputed in either the BS×PIO or RB×BS populations, likely due to the low number of raw SNPs in these regions. We infer that the 'Black Splendor' cultivar may be identical-by-descent for portions of chr8.

3.4. Transmission and correlations of phenological traits

The results showed that none of the traits followed a normal distribution pattern within any of the three families (Table S9). Notably, a significant proportion of seedlings across the three progenies exhibited transgressive values beyond those of their parents for the most of traits (Fig. S1-S3).

The BSxPIO progeny exhibited the earliest flowering among the studied populations, with a considerable number of individuals flowering earlier than both parental genotypes, BS and PIO. Depending on the year, full flowering in some seedlings occurred between January 20th and February 5th (Julian days 20 to 36) (Fig. S1, Fi. S4A, Table S9). In contrast, the progenies of RBxBS and RBxSRP initiated flowering in mid-February, between Julian days 41 and 47. The majority of individuals in both populations exhibited delayed flowering compared to their respective parental genotypes (Fig. S2, Fig. S4A, Table S9). Notably, the RBxSRP progeny exhibited the latest flowering time among the studied populations. Most genotypes within this progeny reached full flowering starting from February 25th (Julian day 55) and extending into the first or second week of March, depending on the year (Fig. S3, Fig. S4A, Table S9).

Regarding flowering intensity and productivity, most individuals from the three progenies exhibited lower values than their respective parents, indicating the presence of hybrid weakness for these traits. This is consistent with the fact that the parental genotypes of all three families displayed high flowering intensity and productivity (Fig. S1-S3, Table S9). Nevertheless, the BSxPIO population showed higher flowering intensity and productivity compared to the other two progenies, while RBxSRP exhibited the lowest values overall. In addition, the BSxPIO progeny exhibited a markedly extended fruit development period, lasting approximately five months (Fig. S1, Fig. S4A, Table S9).

The Kruskal-Wallis test revealed significant differences among years for all evaluated traits, except for productivity and flowering intensity, which did not show significant differences in any of the populations (Table S10). Flowering dates differed significantly between years in all progenies, except for flowering onset in the BSxPIO population. According to the pairwise comparison analysis (Table S11), significant differences were found for flowering dates, except between 2019 and 2021 for full bloom and end of flowering in the BSxPIO progeny.

Significant correlations among phenological traits were observed across all three progenies over the three-year study (Fig. S5). In RB×BS and RB×SRP populations, flowering dates (BF, FF, EF) showed strong correlations ($r > 0.74^{***}$), whereas in BS×PIO, only FF and EF were strongly correlated ($r > 0.93^{***}$). Flowering intensity (FI) and productivity (P) were positively correlated in RB×BS ($r = 0.62^{***}$) and RB×SRP ($r = 0.59^{***}$). High correlations ($r > 0.90^{***}$) were also found between FM and FDP in both populations. Notably, inverse correlations between FM/FDP and P, and between flowering dates and FDP, were observed in RB×BS, with FF in 2021 showing the strongest correlation ($r = -0.47^{*}$). In RB×SRP, flowering dates and FM were significantly correlated, especially in 2019 and 2020. Interannual trait consistency was also high (Table S12).

The strongest year-to-year correlations for flowering dates were seen in BS×PIO (r > 0.77***), followed by RB×BS (r > 0.65***) and RB×SRP (r > 0.51***). FI showed high interannual stability in RB×BS (r = 0.99****), RB×SRP (r > 0.86****), and to a lesser extent in BS×PIO (r > 0.41****). RD, FDP, and P exhibited consistently high correlations across years in all progenies (r > 0.81****) (Table S12).

Principal component analysis (PCA) of phenological traits (Fig. S4A) revealed key patterns of variation among the plum progenies. The first two components, PC1 and PC2, explained 37.8% and 22.4% of the total variance, respectively. The scree plot (Fig. S4B) showed that the first four components together accounted for over 80% of the observed variance. Flowering traits (BF, FF, EF) were the main contributors to PC1, while RD and FDP predominantly influenced PC2. PC3 was primarily shaped by FI and P, highlighting their distinct contribution to phenotypic variation.

3.3. Linkage mapping

Genetic linkage maps were independently constructed for each parent across the three F_1 Japanese plum populations using SNP markers filtered for quality (biallelic, MAF > 0.05, and less than 40 percent missing data) (Table S13).

In the BS×PIO population, 252 SNPs were mapped for the Black Splendor (BS) parent and 519 for the Pioneer (PIO) parent, resulting in 9 linkage groups (LGs) for BS and 13 for PIO (Fig. 3). The BS map spanned 707.78 centimorgans (cM), with LG2 as the longest (175.08 cM), while PIO had a shorter map (417.64 cM) with higher marker density (0.71 cM per SNP) and fragmentation in LG1, LG7, and LG8 (Table 1).

Table 1. Distribution of SNPs across linkage groups for each parent in the F₁ 'Black Splendor' × 'Pioneer' population.

	LG	SNPs	Total distance (cM)	SNP density (cM/SNP)	Maximum gap (cM)
Black Splendor	1	39	87.71	2.25	8.01
	2	26	175.08	6.73	17.38
	3.1	23	33.17	1.44	15.05
	3.2	19	9.67	0.51	3.72
	4	30	132.61	4.42	9.07
	5	54	137.75	2.55	13.83
	6	38	45.56	1.20	7.95
	7.1	13	14.18	1.09	4.11
	7.2	10	72.05	7.20	33.93
	8	0			
	Total	252	707.78	3.04	
Pioneer	1.1	64	40.08	0.63	11.37
	1.2	38	24.36	0.64	6.71
	2	82	94.32	1.15	10.41
	3	45	34.06	0.76	6.30
	4	69	81.11	1.18	10.00
	5	46	34.47	0.75	3.15
	6	7	4.29	0.61	2.86
	7.1	12	8.08	0.67	5.62
	7.2	33	34.78	1.05	14.01
	7.3	15	0.85	0.06	0.42
	8.1	10	4.84	0.48	3.44
	8.2	43	23.69	0.55	5.29
	8.3	55	32.73	0.60	2.92
	Total	519	417.64	0.71	

For the RB×BS population, 441 SNPs were mapped for the Red Beaut (RB) parent and 334 for BS (Fig. 4). The RB map comprised 15 LGs with multiple unlinked segments in LG1, LG4, and LG8, covering 494.79 cM. In contrast, BS displayed 9 LGs spanning 769.81 cM, with lower marker density (2.17 cM per SNP) (Table 2).

Table 2. Distribution of SNPs across linkage groups for each parent in the F₁ 'Red Beaut' × 'Black Splendor'.

У	LG	SNPs	Total distance (cM)	SNP density (cM/SNP)	Maximum gap (cM)
Red Beaut	1.1	24	18.02	0.75	3.85
	1.2	6	2.14	0.36	0.63
	1.3	44	35.09	0.80	23.06
	2	33	65.54	1.99	8.12
	3	55	88.92	1.62	24.80
	4.1	35	19.24	0.55	5.98
	4.2	23	17.50	0.76	2.99
	5.1	17	8.52	0.50	8.40
	5.2	8	0.99	0.12	0.59
	5.3	24	15.17	0.63	1.58
	6	25	23.98	0.96	3.50
	7	63	118.35	1.88	17.28

	Total	334	769.81	2.17	
	8	0			
	7	50	67.04	1.34	12.56
	6	47	168.80	6.26	21.80
	5	58	103.94	1.79	10.65
	4	0			
	3.3	28	42.53	1.52	22.77
	3.2	29	76.20	2.63	26.49
	3.1	22	6.00	0.27	1.94
	2	64	103.24	1.61	9.69
•	1.2	25	55.83	2.23	5.43
Black Splendor	1.1	11	20.88	1.90	4.55
	Total	441	494.79	0.85	
	8.2	8	1.00	0.12	0.55
	8.3	57	73.34	1.29	29.70
	8.1	19	6.99	0.37	2.71

In the RBxSRP population, 428 SNPs were mapped for RB and 305 for SRP (Fig. 5). The RB map had 11 LGs, including segmented LG2, LG5, and LG6, and spanned 646.26 cM. The SRP map extended to 909,23 cM with lower marker density (4.37 cM per SNP) and a large gap in LG4 (20.08 cM) (Table 3).

Table 3. Distribution of SNPs across linkage groups for each parent in the F1 'Red Beaut' × 'Santa Rosa Precoz'.

			Total distance	SND doneity	Maximum gan
	LG	SNPs	(cM)	SNP density (cM/SNP)	Maximum gap (cM)
Red Beaut	1	66	89.47	1.36	16.98
	2.1	31	47.19	1.52	10.35
	2.2	7	24.54	3.51	12.95
	3	61	152.27	2.50	16.00
	4	52	116.35	2.24	10.37
	5.1	45	62.60	1.39	15.60
	5.2	12	10.08	0.84	3.01
	5,3	14	5.99	0.43	1.11
	6.1	44	64.25	1.46	20.15
	6.2	33	24.22	0.73	3.07
	7	0			
	8	63	49.29	0.78	4.05
	Total	428	646.26	1.52	
Santa Rosa	1.1	13	82.40	6.34	17.63
Precoz Y	1.2	17	77.11	4.54	12.03
	2.1	14	11.40	0.81	2.51
	2.2	19	25.52	1.34	7.02
	2.3	17	12.34	0.73	2.11
	3	94	158.35	1.68	12.45
	4	13	149.37	11.49	20.08
	5	53	139.37	2.63	16.01
	6	42	57.85	1.38	14.87
	7	13	105.98	8.15	13.49
	8	10	89.54	8.95	16.29
	Total	305	909.23	4.37	

3.4. Identification of QTLs linked to phenological traits

Using the Kruskal-Wallis test, a total of 113 QTLs were identified across the three F_1 families for the phenological traits evaluated, of which 60 were considered stable.

Flowering Phases (BF, FF, EF)

A total of 53 QTLs were detected—22 for full flowering (FF), 17 for end of flowering (EF), and 14 for beginning of flowering (BF), with 18 classified as stable (Tables S14–S16). The RB×BS population contributed the most QTLs (32 total, 12 stable), followed by RB×SRP (15 total, 3 stable) and BS×PIO (6 total, 3 stable). Stable QTLs were mainly located on LG6 (5 QTLs), LG4 (4), LG3 (3), and LG2 (2) (Fig. 6–8). Most SNPs associated with stable QTLs linked to different flowering dates exhibited a significant allelic effect over the three years of study, predominantly associated with a delayed flowering time (Tables S17, S18 and S19). Notably, SNP S6_32102679 on LG6 (in BS, RB×BS family) was highly associated with FF (KW = 24.05, p<0.0001) (Table S18). Individuals carrying the "T" allele showed delayed FF compared to those with "CC" genotype (Fig. S6). In contrast, for SNP S3_22540873 (LG3.3, BS in RB×BS), the "G" allele was linked to earlier BF (Fig. S7).

Flowering Intensity (FI)

Ten QTLs were associated with FI, of which nine were stable. RBxBS and BSxPIO each contributed 5 and 3 stable QTLs, respectively, while RBxSRP contributed two (one stable). Stable QTLs were distributed across most LGs except LG3 and LG8 (Tables S14–S16). In RBxBS, the most significant QTL was on LG2 (RB), with SNP S2_1349597 showing that the "C" allele increased flowering intensity (Fig. S8). For PIO (BSxPIO), stable QTLs were found on LG4 and LG7. SNPs such as S4_26258734 and S7_10737280 were associated with higher FI, while S7_20461521 showed a negative effect of the "A" allele (Table S17).

Ripening Date (RD) and Fruit Development Period (FDP)

Sixteen QTLs were identified for RD (11 stable), and 18 for FDP (12 stable). BS×PIO and RB×BS contributed the most stable QTLs. Stable RD QTLs were mostly located on LG1 and LG4. The most significant RD QTL was found on LG4.2 of RB (RB×BS) (Table S15), with SNP S4_25017134 showing earlier ripening in "A" allele carriers (Table S18). Another RD QTL on LG4 in RB (RB×SRP) involved SNP S4_19494943, where the "T" allele delayed ripening (Fig. S9, Table S19). For FDP, LG4 showed the highest number of stable QTLs. The most significant FDP QTL overlapped with the RD QTL above, with the "T" allele of S4_19494943 linked to longer development (Table S19).

Productivity

Sixteen QTLs were detected for productivity, 10 of which were stable. BSxPIO contributed the most (9 QTLs, 6 stable), followed by RBxBS (4 stable QTLs). No stable QTLs were found in RBxSRP. Stable QTLs were distributed across LG1 to LG7 (except LG8), with LG2, LG4, and LG5 contributing the highest numbers (Tables S14–S16). The most significant productivity QTL was located on LG1 of BS (BSxPIO), where SNP S1_21058354 showed that the "G" allele conferred higher productivity compared to the "AA" genotype (Table S17).

4. Discussion

This study presents one of the first comprehensive genome-wide analyses of phenological traits in Japanese plum (Prunus salicina), integrating highcoverage WGS of parents and low-coverage WGS (IcWGS) of progenies to construct linkage maps and identify QTLs associated with key traits. This hybrid strategy can help reduce some challenges associated with Ic-WGS such as genotype misclassification or sequencing errors being erroneously classified as genetic variants [46]. In addition, this strategy proved to be highly cost-effective and well-suited for implementation in new breeding programs. The total genotyping costs for the progeny were maintained below \$6 per individual. These costs are consistent with other cost-efficient methods, such as Skim-seq, which reports per-sample genotyping costs below \$3 [47]. In terms of cost per sample, and for the construction of genetic maps in medium-size breeding populations, this strategy is considerably cheaper than traditional SNP arrays, for example, the 60K array developed for almond costs approximately 33 € per sample, even for consortium members (H. Duval pers. comm). Other strategies such as GBS typically around \$30 per sample depending on depth and multiplexing level [34].

In this study, we present, for the first time, genetic linkage maps for Japanese plum constructed using the *Prunus salicina* 'Sanyueli' reference genome. A limited number of genetic linkage maps have been published for Japanese plum, all derived from F₁ populations (Table S20). Among the maps generated, 'Santa Rosa Precoz' yielded the longest (909.23 cM) with a marker density of 4.37 cM per marker, except for the 'Santa Rosa' male parent in [48], which reached 1349.6 cM albeit with lower marker resolution (16.1 cM/marker). However, all these previous maps were aligned to the peach reference genome. More recently, Battistoni et al. [19] enhanced the maps of '98–99' and 'Angeleno' by aligning them to the *Prunus salicina* 'Sanyueli' v2.0 reference genome. Overall, the genetic maps developed in this study demonstrate high quality and resolution, while being generated through a cost-effective approach, making them valuable resources for Japanese plum breeding programs.

Phenological evaluation across the three progenies revealed broad variability, with many seedlings displaying transgressive values beyond parental ranges. This reflects the impact of genetic background, hybridization, and self-incompatibility in enhancing heterozygosity and generating phenotypic extremes in Japanese plum [51,52]. Such diversity also explains the negative heterosis observed for flowering intensity and productivity, where most offspring underperformed compared to parents—a trend consistent with other *Prunus* species like sweet cherry and almond [53,54]. Additionally, productivity may have been influenced by the use of commercial rootstocks in parental trees, known to affect vigor and yield [55]. Similar transgressive patterns have been reported in apricot for phenology and fruit quality traits [56], highlighting the complex inheritance and influence of genetic diversity.

Although most phenological traits showed significant differences across years, the correlation coefficients between years were consistently high. This suggests that, while environmental conditions influence phenology, as previously reported for Japanese plum [11], the strong interannual correlations point to a substantial genetic effect governing the expression of these phenological traits, despite the significant environmental influence. Salazar et al. [11] observed

interannual correlations for bloom date in Japanese plum that were lower than those found in the present study, with Pearson correlation coefficients ranging from 0.49 to 0.59 (p < 0.0001). Additionally, for ripening date, the highest interannual correlation they reported ranged between 0.69 and 0.78, values that are lower than those observed in our three populations (0.959, p-value < 0.001). This interannual variability in phenological traits is influenced by varying climatic conditions each year, particularly temperature, which affects winter chilling accumulation. The differences in chilling accumulation and its dynamic variation between years contribute to the observed phenological differences, as noted by other researchers [54,57]. Moreover, many of the evaluated traits exhibited substantial and significant interannual correlations, further supporting the idea that genetic factors play a significant role in phenological expression, despite environmental effects.

Additionally, high correlation coefficients were observed between RD and FDP, with coefficients exceeding 0.90*** in the RB×BS and RB×SRP populations over the three years of evaluation. Similar correlations were reported by [14] in Japanese plum, with RD and FDP showing correlation coefficients greater than 0.75. In the RB×SRP population, flowering date (FD) was significantly correlated with RD throughout the three years. Specifically, the years 2019 and 2020 showed the highest correlations, with values of 0.44*** in 2019 and 0.47*** in 2020, suggesting that later flowering in the genotypes results in delayed ripening. This correlation has also been reported in Japanese plum by [15] in the '98-99' × 'Angeleno' population.

To date, research on QTLs linked to phenological traits in Japanese plum species has been limited, as most studies have focused on fruit quality traits [15]. As a result, information on the genetic architecture of these phenological traits is scarce, highlighting the importance of the present study. In this study, we successfully identified a large number of QTLs associated with phenology and investigated the allelic effects of significant markers. This analysis enabled the identification of significant SNPs linked to regions associated with phenological traits, which could be used in marker-assisted selection.

The results obtained regarding the QTLs associated with flowering dates (BF, FF, and EF) across the three populations highlight the considerable complexity of this trait. In the BS×PIO population, the most statistically significant QTLs associated with BF were located in the LG3.1 of BS, as well as in LG3 and LG4 of PIO. These two candidate regions in PIO may contribute to the unique lack of correlation between BF and both FF and EF, suggesting a distinct genetic architecture underlying BF in this population. This is likely attributable to alleles inherited from PIO, which is characterized by a notably low chilling requirement approximately 334 chill units or 22 chill portions [58]. Conversely, within the RBxBS population, the most notable QTLs for FF were identified in the LG1.3 of RB and LG6 of BS. The comparison of the QTLs identified in the four progenitors further emphasizes the diverse genetic regions involved, reinforcing the hypothesis that the expression of flowering time is influenced by multiple genes. This finding is consistent with previous studies on species such as peach, sweet cherry, and apricot [59], which also suggest that flowering time is a polygenic trait with complex genetic control. One previous study focused on identifying flowering-related QTLs in Japanese plum and successfully detected QTLs on LG1, LG6, and LG7 [15]. Furthermore, Salazar et al. [60] used SNP-based Genome-Wide Association Studies (GWAS) with GBS to identify markers associated with flowering date in Japanese plum. Additionally, Branchereau et al. [61] evaluated the traits of flowering onset, full bloom, and end of flowering in two populations of sweet cherry, detecting QTLs for these traits in nearly all linkage groups across both populations. The complex genetic control of flowering has also been clearly confirmed here, with the most significant markers located in the terminal region of LG1 and the middle region of LG7, while LG4, LG6, and LG8 also showed correlations with flowering date. Through the detection of candidate genes, this study confirms and expands previous knowledge in Japanese plum about flowering.

Regarding flowering intensity, studies identifying QTLs in *Prunus* species have been limited to date. In the present study, we have revealed the presence of QTLs associated with flowering intensity in various genomic regions, depending on the population under investigation. In the BS×PIO population, significant QTLs were identified in the PIO parent on LG4, associated with flowering onset, as well as in two segments of LG7. In the 'RB×BS' population, QTLs were located on LG1.1, LG2, LG4.2, LG6, and LG8.2, with the most significant QTL found on LG2 of the RB parent, overlapping with both flowering and productivity traits. The most important QTLs for BS were found on LG1.2, associated with productivity, and on LG6, linked to flowering. A previous study by Sánchez-Pérez et al. [54] identified a QTL for flowering intensity in almond, specifically on LG4; however, this QTL exhibited very low significance, explaining less than 12% of the phenotypic variance, and was therefore not considered a major QTL.

Concerning the identification of QTLs associated with RD and FDP, significant findings were observed across the three populations. The female parental lines—BS in BS×PIO, RB in RB×BS, and RB in RB×SRP—all exhibited highly significant QTLs for both RD and FDP on LG4. These results align with previous studies on Japanese plum [4,15] and other *Prunus* species such as peach, apricot, and sweet cherry [59,62], where LG4 has consistently been identified as a crucial genomic region regulating these traits. In contrast, the male parental lines displayed a greater diversity of linkage groups with significant QTLs, with the most notable being two segments of LG1 (LG1.1 and LG1.2) and LG2 in PIO, LG3.3 and LG5 in BS, and LG1.1 in SRP. Furthermore, it is noteworthy that, across most linkage groups, the QTLs associated with RD and FDP often exhibit spatial overlap, as indicated by their shared confidence intervals.

Regarding productivity, QTLs were identified in different genomic regions, depending on the specific population. In the BSxPIO population, the most significant QTL was located on LG1, while in the PIO parent, QTLs associated with productivity were found on LG5. In the RBxBS population, the most significant QTLs were located on LG2 and LG4.1 in RB, while in BS, the second segment of LG1 showed the most notable QTLs, similar to the findings in the first population. The RBxSRP population was the only one where no consistent QTLs were detected across the three years, perhaps due to some limitation in the genetic architecture caused by the genetic origin of both parents. Variability in the localization of QTLs across linkage groups has also been reported in other studies. Sánchez-Pérez et al. [54] identified a QTL for productivity on LG4 in

almond, though its significance was highly irregular, explaining a very low percentage of the phenotypic variance. In peach, QTLs related to productivity have been identified in various linkage groups, such as LG8 [63] and LG6 [64]. These findings, therefore, underscore the complexity and variability of the genetic factors influencing productivity in *Prunus* species.

The prediction of the effects of all significant SNPs associated with the most conserved QTLs (present in at least two years) was performed using SnpEff [65]. The 95 unique SNPs produced a total of 236 predicted effects. Of these, 212 (89.83%) had modifier impact, 11 (4.66%) had moderate impact, and 13 (5.51%) had low impact (Table S21). The largest number of effects was detected for full flowering (FF) time, with 62 effects. A list of candidate genes associated with our target traits was identified. Some can be considered priority candidates for marker development, such as ethylene receptors, heat shock transcription factors, and shikimate hydroxycinnamoyl transferase (HCT). The enzyme shikimate O-hydroxycinnamoyl transferase [EC:2.3.1.133] was affected by a SNP located in a stable QTL for BF and plays a critical role in the phenylpropanoid pathway during seed-plant development [66]. In transgenic alfalfa lines in which HCT levels were severely down-regulated, significant stunting, reduced biomass, and delayed flowering were observed [67].

For FF, significant SNPs affected several ethylene receptors, for example ethylene receptor [EC:2.7.13.-], and EREBP-like factors. EREBPs, together with AP2 (APETALA2), compose the AP2/EREBP superfamily, one of the largest groups of plant-specific transcription factors. They play vital roles in plant growth and development and in responses to diverse stresses including extreme temperatures, drought, high salinity, and pathogen infection [68]. Other enzymes affected by significant SNPs were methionine-cycle or MTA (Yang cycle) enzymes, specifically 5-methylthioribose kinase and methionine synthase, which supply ethylene precursors [69,70]. In addition, Rab11A-dependent tip-focused trafficking and acyl-CoA synthetase functions provision sporopollenin and lipid-derived aroma and support pollination and volatile emission [71,72].

For EF, the same significant SNP S8_27668999 detected for FF affected the ethylene receptor or EREBP-like factor. In addition, another significant SNP affected the regulator of nonsense transcripts 3 (UPF3). In *Arabidopsis*, loss of the core NMD proteins UPF1 and UPF3 leads to late flowering, which suggests that the nonsense-mediated mRNA decay surveillance system can epigenetically modulate flowering time [73].

A common significant SNP across all flowering dates, S4_28542930, located in a stable QTL on chromosome 4, had a modifier effect on carboxy-terminal domain (CTD) RNA polymerase II polypeptide A small phosphatase [EC:3.1.3.16]. This CTD small phosphatase dephosphorylates the RNA polymerase II C-terminal domain. CTD small phosphatases, such as CPL1 and CPL3, act as regulatory switches in flowering control by modulating CTD phosphorylation and by interacting with key flowering repressors such as FLOWERING LOCUS C (FLC) [74-76]. Through these actions, CTD small phosphatases integrate signals that finely regulate flowering time and ensure flowering at appropriate developmental stages and under suitable environmental conditions [74-76]. In *Prunus* species, especially Japanese plum (*Prunus salicina*), there is no previous evidence that specifically links CTD phosphatases to flowering regulation as described in *Arabidopsis*.

For Productivity, the significant SNP S1_27714189 showed an effect on urease [EC:3.5.1.5], a nickel enzyme that hydrolyzes urea into ammonia and carbamate, which then forms carbonic acid and ammonia. In perennial fruit trees such as apple and peach, urease activity hydrolyzes foliar-applied urea into usable nitrogen. This enhances nitrogen remobilization, vegetative growth, and ultimately fruit yield efficiency [77,78].

For ripening date, the significant SNP S1_39702792 affected a heat shock transcription factor. Heat shock transcription factors regulate the expression of heat shock proteins in response to diverse stimuli [79], including cold, drought, and salinity, and during developmental processes such as embryogenesis, germination, and fruit development [80-82]. Same significant SNP affected an carlactone C-19 oxidase [EC:1.14.-.-] enzyme. This enzyme belongs to the cytochrome P450 family, specifically a MAX1 homolog, that oxidizes carlactone (CL) to carlactonoic acid, a key step in strigolactone biosynthesis. In woodland strawberry (a non-climacteric fruit), strigolactone biosynthetic and signaling genes—including MAX1 homologs—are highly expressed during early fruit development but decline sharply at ripening onset, and low or no expression was detected in ripening fruits [83].

Another significant SNP for RD, S1_53963445, affected chloride channel 7 (CLCN7). The CLC family is expressed on internal membranes of plant cells and functions as essential chloride exchangers or channels. Although no studies in Japanese plum or other fruit species currently implicate CLCN7 directly in ripening, CLCs play key roles in ion homeostasis, osmotic regulation, and vacuolar storage. Moreover, chloride can enhance sugar metabolism and fruit sweetness in tomato by stimulating specific metabolic enzymes during fruit development and ripening [84].

Finally, although additional studies are required to rigorously demonstrate SNP-trait associations in Japanese plum, the candidate-gene information reported here provides a useful resource for the *Prunus salicina* research community and may guide future research in this species. In the case of flowering intensity or fruit development period (FDP) the candidates seems of lower-priority and additional studies must be completed to better understand the genetic complexity of these traits.

5. Conclusions

These findings provide valuable genetic and genomic resources for Japanese plum and identify strong candidate markers for the future application of marker-assisted selection in breeding programs. This study presents an innovative and cost-effective strategy for QTL identification related to phenological traits in *Prunus*, based on the integration of high-coverage and low-coverage whole-genome sequencing (lcWGS) in both parental and progeny populations. Trait correlations, together with principal component analysis, offered meaningful insights into the relationships among phenological traits and the genetic mechanisms underlying their expression. Genetic linkage maps were successfully developed for all parental lines across three populations, enabling efficient QTL detection at a significantly lower cost than traditional approaches such as AFLP, GBS, or SLAF-seq. Notably, the most significant SNPs showed consistent and stable allelic effects across three years, reinforcing their potential

as molecular markers to support future breeding in Japanese plum. In addition, we nominate a biologically plausible set of candidate genes within stable QTLs as testable hypotheses. These candidates require genetic and functional validation in *Prunus salicina*, but they provide immediate targets for functional studies and future marker development for Japanese plum breeding.

Competing interests

No competing interest is declared.

Author contributions statement

MNA, PJMG and DR designed the project and edited the first draft of the manuscript. MNA and AG collected data. MNA performed statistical and genetic analyses. PJMG performed the genome and genetic analyses. PJB performed the resequencing analysis. MR, PJB, AG, DR and PMG wrote and revised the manuscript. MNA and PJMG revised and finalized the manuscript. All authors contributed to the article and approved the submitted version

Acknowledgments

We gratefully acknowledge the CEBAS-CSIC/IMIDA Japanese plum breeding program, directed by Dr. Ruiz and Dr. Guevara, for providing the plant material used in this study. This work was supported by the project number 48675: Genetic improvement of agricultural species of interest to the Region of Murcia, Subproject: GI Fruit trees, financed by ERDF21-27 and by the AGROALNEXT programme and was supported by MCIN with funding from European Union NextGenerationEU (PRTR-C17.I1) and by Fundación Séneca with funding from Comunidad Autónoma Región de Murcia (CARM). María Nicolás-Almansa was supported by a PhD fellowship (FPU16/03896) from the Spanish Ministry of Economy, Industry and Competitiveness (MINECO).

728729 Data availability

The genome sequencing data for this publication have been deposited to the NCBI BioProject database (http://www.ncbi.nlm.nih.gov/bioproject/1282032) under accession number PRJNA1282032.

7. References

- [1] FAOSTAT. (2022). Food and agriculture organization. Agricultural statistics database. FAO. https://www.fao.org/faostat/es/#home
- [2] Okie, W. R., & Ramming, D. W. (1999). Plum breeding worldwide. HortTechnology, 9(2), 162–176. https://doi.org/10.21273/horttech.9.2.162
- [3] van Nocker, S., & Gardiner, S. E. (2014). Breeding better cultivars, faster: applications of new technologies for the rapid deployment of superior horticultural tree crops. *Horticulture Research*, 1, 14022. https://doi.org/10.1038/hortres.2014.22
- [4] Salazar, J. A., Pacheco, I., Shinya, P., Zapata, P., Silva, C., Aradhya, M., Velasco, D., Ruiz, D., Martínez-Gómez, P., & Infante, R. (2017). Genotyping by sequencing for Snp-Based linkage analysis and identification of QTLs linked to fruit quality traits in japanese plum (*Prunus salicina* lindl.). *Frontiers in Plant Science*, 8(April), 1–14. https://doi.org/10.3389/fpls.2017.00476

- [5] Liu, W., Liu, N., Yu, X., Sun, M., Zhang, Y., Xu, M., Zhang, Q., & Liu, S. (2013).
 PLUM GERMPLASM RESOURCES AND BREEDING IN LIAONING OF
 CHINA. Acta Horticulturae, 985, 43–46.
 https://doi.org/10.17660/ActaHortic.2013.985.4
- 753 [6] Ruiz, D., Cos, J., Egea, J., García, F., Nortes, M. D., Carrillo, A., & Guevara, 754 A. (2019). Progress in the Japanese plum (*Prunus salicina* L.) breeding 755 program developed by CEBAS-CSIC and IMIDA in Murcia, Spain. *Acta Horticulturae*, 1260, 47–48. https://doi.org/DOI: 757 10.17660/ActaHortic.2019.1260.9
- 758 [7] Petri, C., Ruiz, D., Faize, M., Burgos, L., & Alburquerque, N. (2020). *Prunus*759 *domestica* plum. *CABI*, 512–531.
 760 https://doi.org/10.1079/9781780648279.0512.

- [8] Fernandez, E., Whitney, C., Cuneo, I. F., & Luedeling, E. (2020). Prospects of decreasing winter chill for deciduous fruit production in Chile throughout the 21st century. *Climatic Change*, 159(3), 423-439.
- [9] Fernandez, E., Mojahid, H., Fadón, E., Rodrigo, J., Ruiz, D., Egea, J. A., Ben Mimoun, M., Kodad, O., El Yaacoubi A., Ghrab M., Egea J., Benmoussa H., Borgini N., Elloumi O., & Luedeling E. (2023). Climáte change impacts on winter chill in Mediterranean temperate fruit orchards. Regional environmental change, 23(1), 7.
- [10] Rodríguez, A., Pérez-López, D., Sánchez, E., Centeno, A., Gómara, I., Dosio, A., & Ruiz-Ramos, M. (2019). Chilling accumulation in fruit trees in Spain under climate change. *Natural Hazards and Earth System Sciences*, 19(5), 1087-1103.
- [11] Guerrero, B. I., Fadón, E., Guerra, M. E., & Rodrigo, J. (2024). Perspectives on the adaptation of Japanese plum-type cultivars to reduced winter chilling in two regions of Spain. *Frontiers in Plant Science*, 15, 1343593.
- [12] Guerra, M. E., & Rodrigo, J. (2015). Japanese plum pollination: A review. *Scientia Horticulturae*, 197(November), 674–686. https://doi.org/10.1016/j.scienta.2015.10.032
- [13] Fiol, A., García-Gómez, B. E., Jurado-Ruiz, F., Alexiou, K., Howad, W., & Aranzana, M. J. (2021). Characterization of Japanese Plum (*Prunus salicina*) PsMYB10 Alleles Reveals Structural Variation and Polymorphisms Correlating With Fruit Skin Color. *Frontiers in Plant Science*, 12(June), 1–17. https://doi.org/10.3389/fpls.2021.655267
- [14] Fiol, A., García, S., Dujak, C., Pacheco, I., Infante, R., & Aranzana, M. J. (2022). An LTR retrotransposon in the promoter of a PsMYB10.2 gene associated with the regulation of fruit flesh color in Japanese plum. *Horticulture Research*, 9(December). https://doi.org/10.1093/hr/uhac206
- [15] Salazar, J. A., Pacheco, I., Zapata, P., Shinya, P., Ruiz, D., Martínez-Gómez,
 P., & Infante, R. (2020). Identification of loci controlling phenology, fruit
 quality and post-harvest quantitative parameters in Japanese plum (*Prunus salicina* Lindl.). *Postharvest Biology and Technology*, 169(June), 111292.
 https://doi.org/10.1016/j.postharvbio.2020.111292
- 793 [16] Valderrama-Soto, D., Salazar, J., Sepúlveda-González, A., Silva-Andrade, C., Gardana, C., Morales, H., Battistoni, B., Jiménez-Muñoz, P., González, M., Peña-Neira, Á., Infante, R., & Pacheco, I. (2021). Detection of Quantitative Trait Loci Controlling the Content of Phenolic Compounds in an Asian Plum (*Prunus salicina* L.) F₁ Population. *Frontiers in Plant Science*, 12. https://doi.org/10.3389/fpls.2021.679059

799 [17] Verde, I., Jenkins, J., Dondini, L., Micali, S., Pagliarani, G., Vendramin, E., Paris, R., Aramini, V., Gazza, L., Rossini, L., Bassi, D., Troggio, M., Shu, S., Grimwood, J., Tartarini, S., Dettori, M. T., & Schmutz, J. (2017). The Peach v2.0 release: High-resolution linkage mapping and deep resequencing improve chromosome-scale assembly and contiguity. *BMC Genomics*, 18(1). https://doi.org/10.1186/s12864-017-3606-9

- [18] Shi, S., Li, J., Sun, J., Yu, J., & Zhou, S. (2013). Phylogeny and Classification of *Prunus sensu* lato (Rosaceae). *Journal of Integrative Plant Biology*, 55(11), 1069–1079. https://doi.org/https://doi.org/10.1111/jipb.12095
- [19] Battistoni, B., Salazar, J., Vega, W., Valderrama-Soto, D., Jiménez-Muñoz, P., Sepúlveda-González, A., Ahumada, S., Cho, I., Gardana, C. S., Morales, H., Peña-Neira, Á., Silva, H., Maldonado, J., González, M., Infante, R., & Pacheco, I. (2022). An Upgraded, Highly Saturated Linkage Map of Japanese Plum (*Prunus salicina* Lindl.), and Identification of a New Major Locus Controlling the Flavan-3-ol Composition in Fruits. *Frontiers in Plant Science*, 13. https://doi.org/10.3389/fpls.2022.805744
- 815 [20] Liu, C., Feng, C., Peng, W., Hao, J., Wang, J., Pan, J., & He, Y. (2020). 816 Chromosome-level draft genome of a diploid plum (*Prunus salicina*). *GigaScience*, *9*(12). https://doi.org/10.1093/gigascience/giaa130
 - [21] Wang, N., Yuan, Y., Wang, H., Yu, D., Liu, Y., Zhang, A., Gowda, M., Nair, S. K., Hao, Z., Lu, Y., San Vicente, F., Prasanna, B. M., Li, X., & Zhang, X. (2020). Applications of genotyping-by-sequencing (GBS) in maize genetics and breeding. *Scientific Reports*, 10(1), 16308. https://doi.org/10.1038/s41598-020-73321-8
- [22] Kumar, P., Choudhary, M., Jat, B. S., Kumar, B., Singh, V., Kumar, V., Singla, D., & Rakshit, S. (2021). Skim sequencing: an advanced NGS technology for crop improvement. *Journal of Genetics*, 100(2), 38. https://doi.org/10.1007/s12041-021-01285-3
 - [23] Navarro, A., Bourke, P. M., van de Weg, E., Clot, C. R., Arens, P., Finkers, R., & Maliepaard, C. (2023). Smooth Descent: A ploidy-aware algorithm to improve linkage mapping in the presence of genotyping errors. Frontiers in Genetics, 14. https://www.frontiersin.org/journals/genetics/articles/10.3389/fgene.2023.1 049988
- 833 [24] Ruiz, D., García-Gómez, B. E., Egea, J., Molina, A., Martínez-Gómez, P., & Campoy, J. A. (2019). Phenotypical characterization and molecular fingerprinting of natural early-flowering mutants in apricot (Prunus armeniaca L.) and Japanese plum (*P. salicina Lindl.*). *Scientia Horticulturae*, 254, 187-192.
- [25] García-Gómez, B., Razi, M., Salazar, J. A., Prudencio, A. S., Ruiz, D., Dondini, L., & Martínez-Gómez, P. (2018). Comparative analysis of SSR markers developed in exon, intron, and intergenic regions and distributed in regions controlling fruit quality traits in *Prunus* species: genetic diversity and association studies. *Plant Molecular Biology Reporter*, 36(1), 23-35.
- [26] Doyle, J.J., & Doyle, J.L., (1987). A rapid DNA insolation procedure for small quantities of fresh leaf tissue. Phytochem Bull, https://worldveg.tind.io/record/33886
- [27] Zimin, A. V., Puiu, D., Luo, M. C., Zhu, T., Koren, S., Marçais, G., Yorke, J.
 A., Dvořák, J., & Salzberg, S. L. (2017). Hybrid assembly of the large and highly repetitive genome of *Aegilops tauschii*, a progenitor of bread wheat,

- with the MaSuRCA mega-reads algorithm. *Genome Research*, *27*(5), 787–792. https://doi.org/10.1101/gr.213405.116
- [28] Gurevich, A., Saveliev, V., Vyahhi, N., & Tesler, G. (2013). QUAST: Quality assessment tool for genome assemblies. *Bioinformatics*, *29*(8), 1072–1075. https://doi.org/10.1093/bioinformatics/btt086
- [29] Langmead, B., Wilks, C., Antonescu, V., & Charles, R. (2019). Scaling read aligners to hundreds of threads on general-purpose processors. Bioinformatics, 35(3), 421–432. https://doi.org/10.1093/bioinformatics/bty648
- 858 [30] Simão, F. A., Waterhouse, R. M., Ioannidis, P., Kriventseva, E. V., & Zdobnov, E. M. (2015). BUSCO: Assessing genome assembly and annotation completeness with single-copy orthologs. *Bioinformatics*, *31*(19), 3210–3212. https://doi.org/10.1093/bioinformatics/btv351

864

871

872

873874

875 876

877

878 879

880

881

- [31] Li, H., & Durbin, R. (2009). Fast and accurate short read alignment with Burrows-Wheeler transform. *Bioinformatics*, *25*(14), 1754–1760. https://doi.org/10.1093/bioinformatics/btp324
- [32] Danecek, P., Bonfield, J. K., Liddle, J., Marshall, J., Ohan, V., Pollard, M. O., Whitwham, A., Keane, T., McCarthy, S. A., & Davies, R. M. (2021). Twelve years of SAMtools and BCFtools. *GigaScience*, 10(2). https://doi.org/10.1093/gigascience/giab008
- 869 [33] Broad Institute. (2019). *Picard Toolkit*. Broad Institute, GitHub Repository. https://broadinstitute.github.io/picard/
 - [34] Poland, J.A., Brown, P.J., Sorrells, M.E., Jannink, J.-L. (2012) Development of high-density genetic maps for barley and wheat using a novel two-enzyme Genotyping-by-Sequencing approach. PLoS ONE 7(2): e32253. https://doi.org/10.1371/journal.pone.0032253
 - [35] Glaubitz, J. C., Casstevens, T. M., Lu, F., Harriman, J., Elshire, R. J., Sun, Q., & Buckler, E. S. (2014). TASSEL-GBS: A high capacity genotyping by sequencing analysis pipeline. *PLoS ONE*, *9*(2). https://doi.org/10.1371/journal.pone.0090346
 - [36] Swarts, K., Li, H., Romero Navarro, J. A., An, D., Romay, M. C., Hearne, S., Acharya, C., Glaubitz, J. C., Mitchell, S., Elshire, R. J., Buckler, E. S., & Bradbury, P.J. (2014). Novel Methods to Optimize Genotypic Imputation for Low-Coverage, Next-Generation Sequence Data in Crop Plants. *The Plant Genome*, 7(3). https://doi.org/10.3835/plantgenome2014.05.0023
- 884 [37] Meier, U., Graf, H., Hack, H., Hess, M., Kennel, W., Klose, R., Mappes, D., 885 Seipp, D., Stauss, R., Streif, J., & Boom, T. V. D. (1994). Phanologische 886 Entwicklungsstadien des Kernobstes (*Malus domestica* Borkh. und Pyrus 887 communis L.). *Nachrichtenbl. Deut. Pflanzenschutzd.*, 46, 141–153.
- [38] IMB Corp. (2020). IBM SPSS Statistics for Windows, Version 27.0. Armonk,NY: IBM Corp.
- 890 [39] Wei, T., & Simko, V. (2021). *R package "corrplot": Visualization of a Correlation Matrix (Version 0.92)*. https://github.com/taiyun/corrplot
- [40] Kassambara, A., & Mundt, F. (2020). *factoextra: Extract and Visualize the*Results of Multivariate Data Analyses. R package version 1.0.7 (R package version 1.0.7). https://CRAN.R-project.org/package=factoextra
- 895 [41] Lê, S., Josse, J., & Husson, F. (2008). FactoMineR: an R package for 896 multivariate analysis. *Journal of Statistical Software*, 25, 1–18. 897 https://doi.org/10.1016/j.envint.2008.06.007

- 898 [42] Van Ooijen, J. W. (2009). MapQTL 6 ® Software for the mapping of quantitative trait loci in experimental populations of diploid species. 900 www.kyazma.nl
- 901 [43] Van Ooijen, J. W. (2011). Multipoint maximum likelihood mapping in a full-902 sib family of an outbreeding species. *Genetics Research*, 93(5), 343–349. 903 https://doi.org/10.1017/S0016672311000279
- 904 [44] Ouellette, L. A., Reid, R. W., Blanchard, S. G., & Brouwer, C. R. (2018). 905 LinkageMapView-rendering high-resolution linkage and QTL maps. 906 Bioinformatics, 34(2), 306–307. 907 https://doi.org/10.1093/bioinformatics/btx576
- 908 [45] Wickham, H. (2016). ggplot2: Elegant Graphics for Data Analysis. Springer-909 Verlag New York. https://ggplot2.tidyverse.org

911

912

913

920

921 922

923

924

925

926

927

928

929 930

931 932

933 934

935

- [46] Baraja-Fonseca, V., Arrones, A., Vilanova, S., Plazas, M., Prohens, J., Bombarely, A., & Gramazio, P. (2025). Benchmarking of low coverage sequencing workflows for precision genotyping in eggplant. *BMC Plant Biology*, 25(1), 1125.
- [47] Adhikari, L., Shrestha, S., Wu, S., Crain, J., Gao, L., Evers, B., Wilson, D., 914 915 Ju, Y., Koo, DH., Hucl, P., Pozniak, C., Walkowiak, S., Wang, X., Wu, J., Glaubitz, J.C., DeHaan, L., Friebe, B &, Poland, J. (2022). A high-916 917 throughput skim-sequencing approach for genotyping, dosage estimation translocations. Sci Rep 12, 918 identifying 17583 (2022).919 https://doi.org/10.1038/s41598-022-19858-2
 - [48] Vieira, E. A., Onofre Nodari, R., Cibele De Mesquita Dantas, A., Henri, J.-P., Ducroquet, J., Dalbó, M., & Borges, C. V. (2005). Genetic mapping of Japanese plum. *Crop Breeding and Applied Biotechnology*, *5*, 29–37. https://www.researchgate.net/publication/220021118
 - [49] Carrasco, B., González, M., Gebauer, M., García-González, R., Maldonado, J., & Silva, H. (2018). Construction of a highly saturated linkage map in Japanese plum (*Prunus salicina* L.) using GBS for SNP marker calling. *PLoS ONE*, 13(12). https://doi.org/10.1371/journal.pone.0208032
 - [50] Zhang, Q. ping, Wei, X., Liu, N., Zhang, Y. ping, Xu, M., Zhang, Y. jun, Ma, X. xue, & Liu, W. sheng. (2020). Construction of an SNP-based high-density genetic map for Japanese plum in a Chinese population using specific length fragment sequencing. *Tree Genetics and Genomes*, 16(1). https://doi.org/10.1007/s11295-019-1385-y
 - [51] Carrasco, B., Meisel, L., Gebauer, M., Garcia-Gonzales, R., & Silva, H. (2013). Breeding in peach, cherry and plum: From a tissue culture, genetic, transcriptomic and genomic perspective. *Biological Research*, 46(3), 219–230. https://doi.org/10.4067/S0716-97602013000300001
- [52] Guerrero, B. I., Guerra, M. E., Herrera, S., Irisarri, P., Pina, A., & Rodrigo, J.
 (2021). Genetic diversity and population structure of japanese plum-type
 (Hybrids of *P. salicina*) accessions assessed by ssr markers. *Agronomy*,
 11(9). https://doi.org/10.3390/agronomy11091748
- 941 [53] Theiler-Hedtrich, R. (1994). Inheritance of tree and fruit characters in 942 progenies from crosses of sweet cherry (*Prunus avium* L.) cultivars. 943 *Euphytica*, 77(1), 37–44. https://doi.org/10.1007/BF02551458
- [54] Sánchez-Pérez, R., Ortega, E., Duval, H., Martínez-Gómez, P., & Dicenta,
 F. (2007). Inheritance and relationships of important agronomic traits in almond. *Euphytica*, *155*(3), 381–391. https://doi.org/10.1007/s10681-006-947

- [55] Jiménez, S., Pinochet, J., Romero, J., Gogorcena, Y., & Moreno, M. Á.
 (2010). Influence of rootstocks on peach productivity, vigor, and nutrient uptake in Mediterranean conditions. *Scientia Horticulturae*, 129(1), 58–63
- [56] Salazar, J. A., Ruiz, D., Campoy, J. A., Tartarini, S., Dondini, L., & Martínez Gómez, P. (2016). Inheritance of reproductive phenology traits and related
 QTL identification in apricot. *Tree Genetics and Genomes*, 12(4).
 https://doi.org/10.1007/s11295-016-1027-6
- [57] Minas, I. S., Tanou, G., & Molassiotis, A. (2018). Environmental and orchard
 bases of peach fruit quality. Scientia Horticulturae, 235, 307–322.
 https://doi.org/10.1016/j.scienta.2018.01.028

- [58] Ruiz, D., Egea, J., Salazar, J. A., & Campoy, J. A. (2018). Chilling and heat requirements of Japanese plum cultivars for flowering. *Scientia Horticulturae*, 242, 164-169.
- [59] Dirlewanger, E., Quero-García, J., Le Dantec, L., Lambert, P., Ruiz, D., Dondini, L., Illa, E., Quilot-Turion, B., Audergon, J. M., Tartarini, S., Letourmy, P., & Arús, P. (2012). Comparison of the genetic determinism of two key phenological traits, flowering and maturity dates, in three *Prunus* species: Peach, apricot and sweet cherry. *Heredity*, 109(5), 280–292. https://doi.org/10.1038/hdy.2012.38.
- [60] Salazar, J. A., Igor, P., Claudia, S., Patricio, Z., Paulina, S., David, R., Pedro, M.-G., & and Infante, R. (2018). Development and applicability of GBS approach for genomic studies in Japanese plum (*Prunus salicina* Lindl.). *The Journal of Horticultural Science and Biotechnology*, 94(3), 284–294. https://doi.org/10.1080/14620316.2018.1543559
- [61] Branchereau, C., Quero-García, J., Zaracho-Echagüe, N. H., Lambelin, L., Fouche, M., Wenden, B., Donkpegan, A., Le Dantec, L., Barreneche, T., Alletru, D., Parmentier, J., & Dirlewanger, E. (2022). New insights into flowering date in *Prunus*: fine mapping of a major QTL in sweet cherry. *Horticulture Research*, 9(July 2021). https://doi.org/10.1093/hr/uhac042
- [62] Rawandoozi, Z. J., Hartmann, T. P., Carpenedo, S., Gasic, K., da Silva Linge, C., Cai, L., Van de Weg, E., & Byrne, D. H. (2021). Mapping and characterization QTLs for phenological traits in seven pedigree-connected peach families. *BMC Genomics*, 22(1). https://doi.org/10.1186/s12864-021-07483-8
- [63] Zeballos, J. L., Abidi, W., Giménez, R., Monforte, A. J., Moreno, M. Á., & Gogorcena, Y. (2016). Mapping QTLs associated with fruit quality traits in peach [Prunus persica (L.) Batsch] using SNP maps. Tree Genetics and Genomes, 12(3). https://doi.org/10.1007/s11295-016-0996-9
- 986 [64] Dirlewanger, E., Moing, A., Rothan, C., Svanella, L., Pronier, V., Guye, A., Plomion, C., & Monet, R. (1999). Mapping QTLs controlling fruit quality in peach (*Prunus persica* (L.) Batsch). *Theoretical and Applied Genetics*, 989 98(1), 18–31. https://doi.org/10.1007/s001220051035
- 990 [65] Cingolani, P., Platts, A., Wang, L. L., Coon, M., Nguyen, T., Wang, L., Land, 991 S. J., Lu, X., & Ruden, D. M. (2012) A program for annotating and predicting 1992 the effects of single nucleotide polymorphisms, SnpEff: SNPs in the genome 1993 of *Drosophila melanogaster strain* w¹¹¹⁸; iso-2; iso-3. *Fly*, 6(2):80–92. 1994 doi:10.4161/fly.19695
- 995 [66] Kriegshauser, L., Knosp, S., Grienenberger, E., Tatsumi, K., Gütle, D. D., 996 Sørensen, I., Herrgott, L., Zumsteg, J., Rose, J. K. C., Reski, R., Werck-997 Reichhart, D., & Renault, H. (2021). Function of the

- 998 HYDROXYCINNAMOYL-CoA:SHIKIMATE HYDROXYCINNAMOYL 999 TRANSFERASE is evolutionarily conserved in embryophytes. *The Plant* 1000 *Cell*, 2;33(5):1472-1491. doi: 10.1093/plcell/koab044.
- [67] Shadle, G., Chen, F., Reddy, M. S., Jackson, L., Nakashima, J., & Dixon, R.
 A. (2007). Down-regulation of hydroxycinnamoyl CoA: shikimate hydroxycinnamoyl transferase in transgenic alfalfa affects lignification, development and forage quality. *Phytochemistry*, 68(11), 1521-1529.
- 1005 [68] Chen, L., Han, J., Deng, X., Tan, S., Li, L., Li, L., Zhou, J., Peng, H., Yang, 1006 G., He, G., & Zhang, W. (2016). Expansion and stress responses of AP2/EREBP superfamily in *Brachypodium Distachyon*. *Scientific Reports*, 6,21623. https://doi.org/10.1038/srep21623
- 1009 [69] Sekowska, A., Ashida, H., & Danchin, A. (2019). Revisiting the methionine salvage pathway and its paralogues. *Microbial Biotechnology* 12(1):77-97. doi: 10.1111/1751-7915.13324.
- 1012 [70] Bürstenbinder, K., Waduwara, I., Schoor, S., Moffatt, B. A., Wirtz, M., Minocha, S. C., Oppermann, Y., Bouchereau, A., Hell, R., & Sauter, M. (2010). Inhibition of 5'-methylthioadenosine metabolism in the Yang cycle alters polyamine levels, and impairs seedling growth and reproduction in Arabidopsis. *The Plant Journal*, 62(6):977-88. doi: 10.1111/j.1365-313X.2010.04211.x.
- 1018 [71] de Graaf, B. H., Cheung, A. Y., Andreyeva, T., Levasseur, K., Kieliszewski, 1019 M., & Wu, H.M. (2005). Rab11 GTPase-regulated membrane trafficking is crucial for tip-focused pollen tube growth in tobacco. *Plant Cell*, 17(9): 2564-1021 79. doi: 10.1105/tpc.105.033183.
- [72] de Azevedo, S. C., Kim S. S., Koch, S., Kienow, L., Schneider, K., McKim, 1022 S. M., Haughn, G. W., Kombrink, E., & Douglas, C. J. (2009). A novel fatty 1023 1024 Acyl-CoA Synthetase is required for pollen development and sporopollenin 1025 biosynthesis in Arabidopsis. Plant Cell, 21(2):507-25. doi: 1026 10.1105/tpc.108.062513.
- [73] Nasim, Z., Fahim, M., Hwang, H., Susila, H., Jin, S., Youn, G., & Ahn, J.H. 1027 1028 (2021) Nonsense-mediated mRNA decay modulates Arabidopsis flowering 1029 via the SET DOMAIN GROUP *40–FLOWERING* LOCUS 1030 C module, Journal of Experimental Botany, 72(20):7049-7066, https://doi.org/10.1093/jxb/erab331 1031
- 1032 [74] Yuan, C., Xu, J., Chen, Q., Liu, Q., Hu, Y., Jin, Y., & Qin, C. (2021). C-1033 terminal domain phosphatase-like 1 (CPL1) is involved in floral transition in 1034 *Arabidopsis. BMC genomics*, 22(1), 642.
- 1035 [75] Zhang, Y., & Shen, L. (2022). CPL2 and CPL3 act redundantly in FLC activation and flowering time regulation in *Arabidopsis*. *Plant Signaling* & Behavior, 17(1), 2026614.
- 1038 [76] Kyung, J., Jeong, D., Eom, H., Kim, J., Kim, J. S., & Lee, I. (2024). C-1039 TERMINAL DOMAIN PHOSPHATASE-LIKE 1 promotes flowering with TAF15b by repressing the floral repressor gene FLOWERING LOCUS C. 1041 Molecules and cells, 47(10), 100114. https://doi.org/10.1016/j.mocell.2024.100114
- 1043 [77] Weinbaum, S. A., Johnson R. S., & DeJong T. M. (1992). Causes and consequences of overfertilization in orchards. *HortTechnology* 2:112–121.
- 1045 [78] Dong, S., Cheng, L., Scagel, C. F., & Fuchigami, L. H. (2002). Nitrogen absorption, translocation and distribution from urea applied in autumn to

leaves of young potted apple (*Malus domestica*) trees. *Tree physiology*, 22(18), 1305-1310.

- [79] Pirkkala, L., Nykänen, P., & Sistonen, L. E. A. (2001). Roles of the heat shock transcription factors in regulation of the heat shock response and beyond. *The FASEB Journal*, 15(7), 1118-1131.
- [80] Wehmeyer, N., Hernandez, L. D., Finkelstein, R. R., & Vierling, E. (1996). Synthesis of small heat-shock proteins is part of the developmental program of late seed maturation. *Plant Physiology*, 112(2), 747-757.
- [81] Almoguera, C., Prieto-Dapena, P., & Jordano, J. (1998). Dual regulation of a heat shock promoter during embryogenesis: stage-dependent role of heat shock elements. *The Plant Journal*, 13(4), 437-446.
- [82] Sun, W., Bernard, C., Van De Cotte, B., Van Montagu, M., & Verbruggen, N. (2001). At-HSP17. 6A, encoding a small heat-shock protein in *Arabidopsis*, can enhance osmotolerance upon overexpression. *The Plant Journal*, 27(5), 407-415.
- [83] Wu, H., Li, H., Chen, H., Qi, Q., Ding, Q., Xue, J., Jiang, X., Hou X., & Li, Y. (2019). Identification and expression analysis of strigolactone biosynthetic and signaling genes reveal strigolactones are involved in fruit development of the woodland strawberry (*Fragaria vesca*). BMC plant biology, 19(1), 73.
- [84] Su, L., Lu, T., Li, Q., Li, Y., Wan, X., Jiang, W., & Yu, H. (2025). Chlorine Modulates Photosynthetic Efficiency, Chlorophyll Fluorescence in Tomato Leaves, and Carbohydrate Allocation in Developing Fruits. *International Journal of Molecular Sciences*, 26(7), 2922.

1075	Tables
1076	

1082

1083 1084

Table 1. Description of each linkage group (LG) for each genitor in the F₁ Japanese plum population 'Black Splendor' × 'Pioneer'.

Table 2. Description of each linkage group (LG) for each genitor in the F₁ Japanese plum population 'Red Beaut' × 'Black Splendor'.

Table 3. Description of each linkage group (LG) for each genitor in the F₁ Japanese plum population 'Red Beaut' × 'Santa Rosa Precoz'.



Figures

Figure 1. Illustrative images of several fruits of each parental genotype and fruits of each population evaluated in this study.

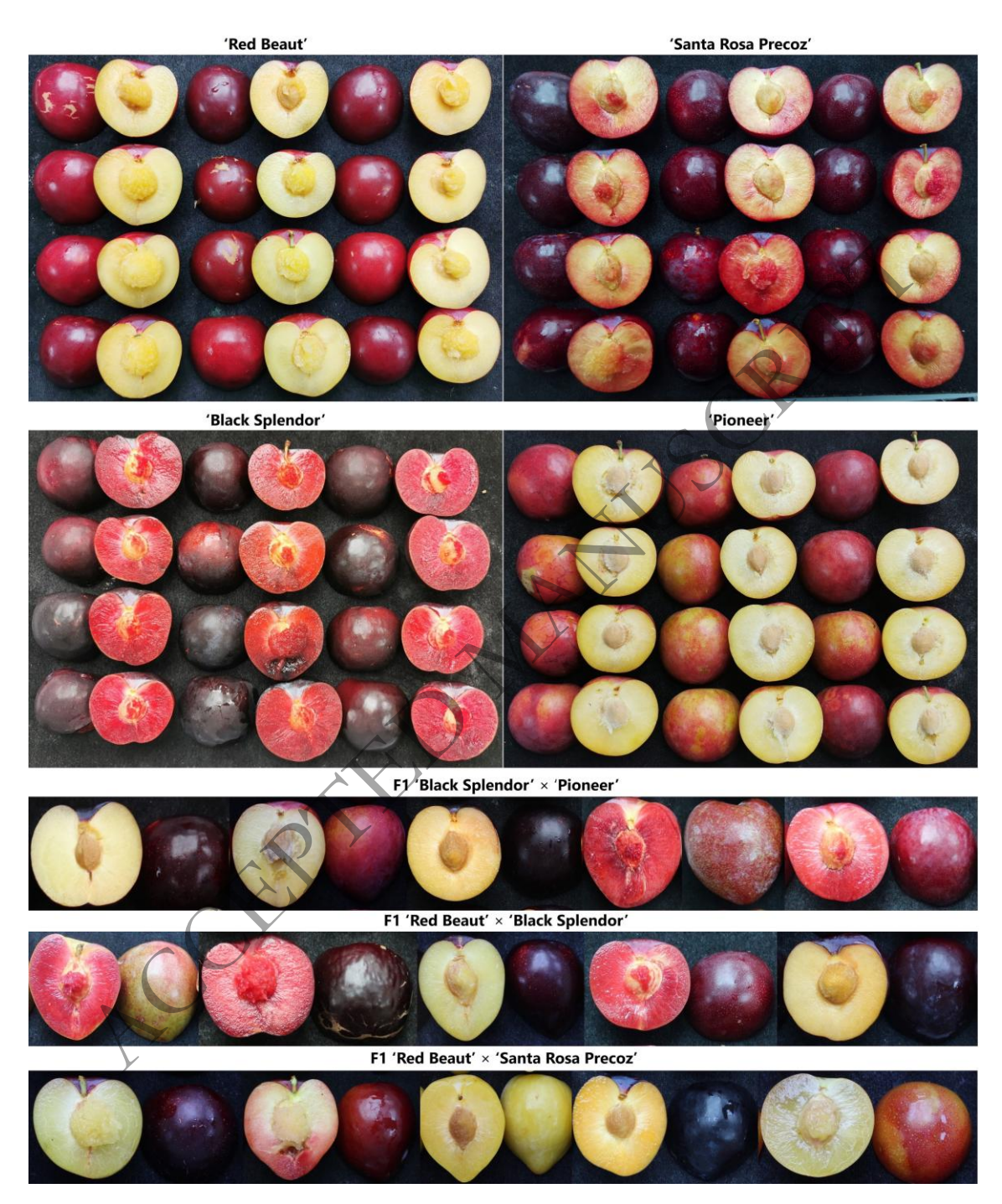


Figure 2. The complete pedigree for each parental genotype. Magenta circle highlights 'Santa Rosa' and its spontaneous mutant 'Santa Rosa Precoz', identified by CSIC technician A. Molina [24]. In blue are the three F_1 Japanese plum populations.

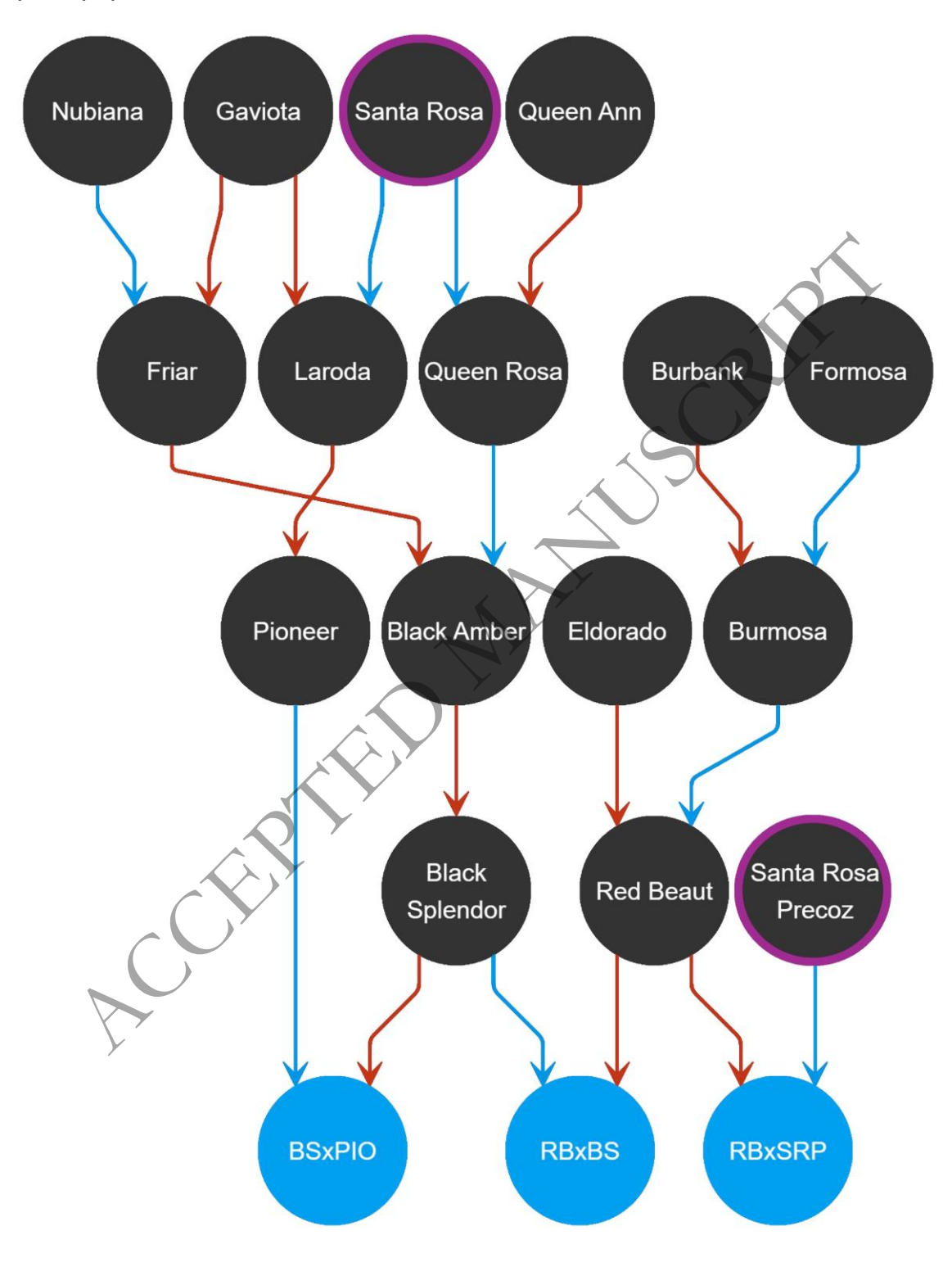


Figure 3. Genetic linkage maps for each genitor in the F₁ Japanese plum population 'Black Splendor' × 'Pioneer'. Markers positions are represented by black lines. The linkage groups of the female progenitor 'Black Splendor' (BS) are indicated in light blue, and those of the male progenitor 'Pioneer' (PIO) are indicated in green.

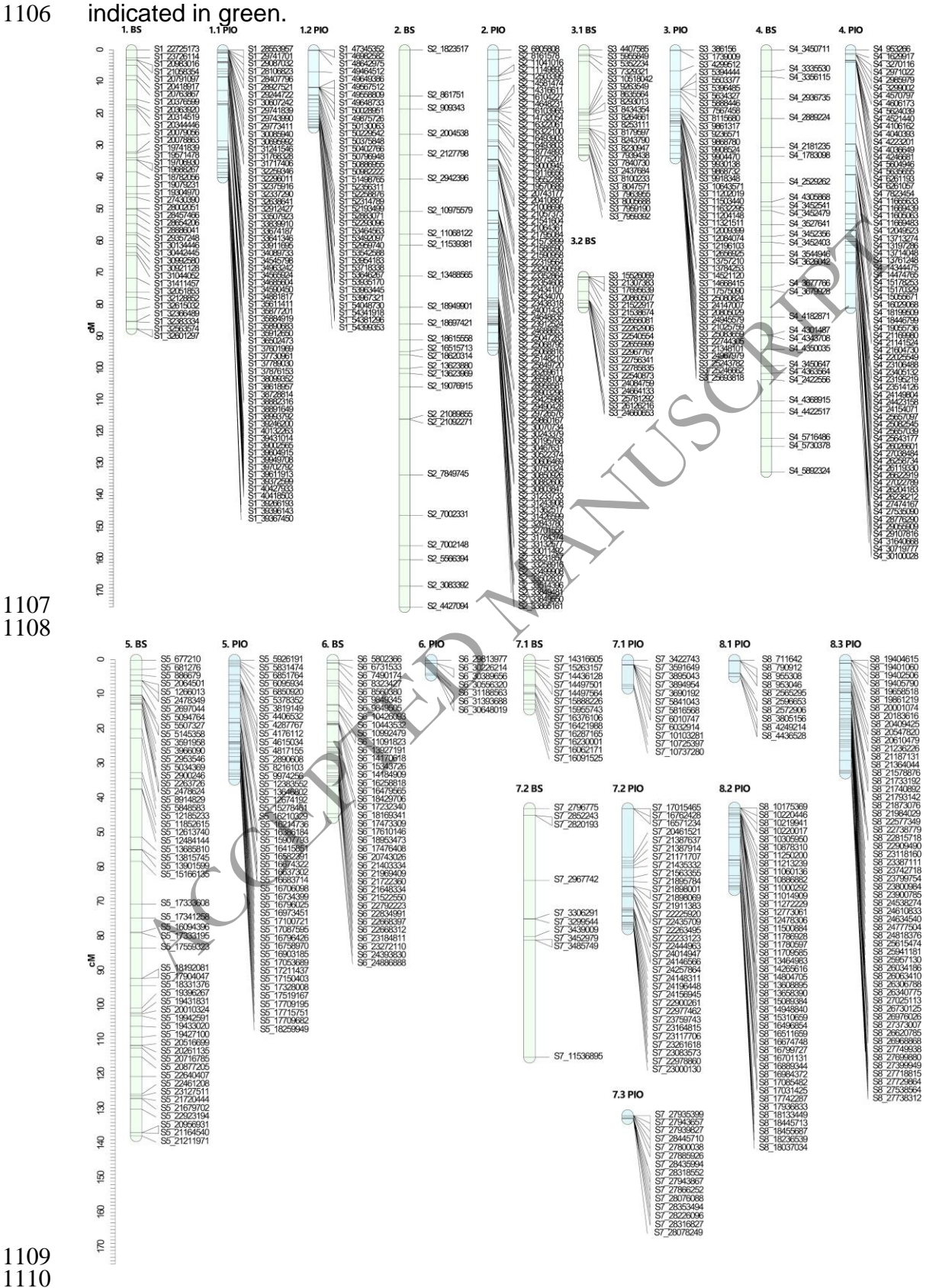


Figure 4. Genetic linkage maps for each genitor in the F_1 Japanese plum population 'Red Beaut' × 'Black Splendor'. Markers positions are represented by black lines. The linkage groups of the female progenitor 'Red Beaut' (RB) are indicated in light blue, and those of the male progenitor 'Black Splendor' (BS) are indicated in green.

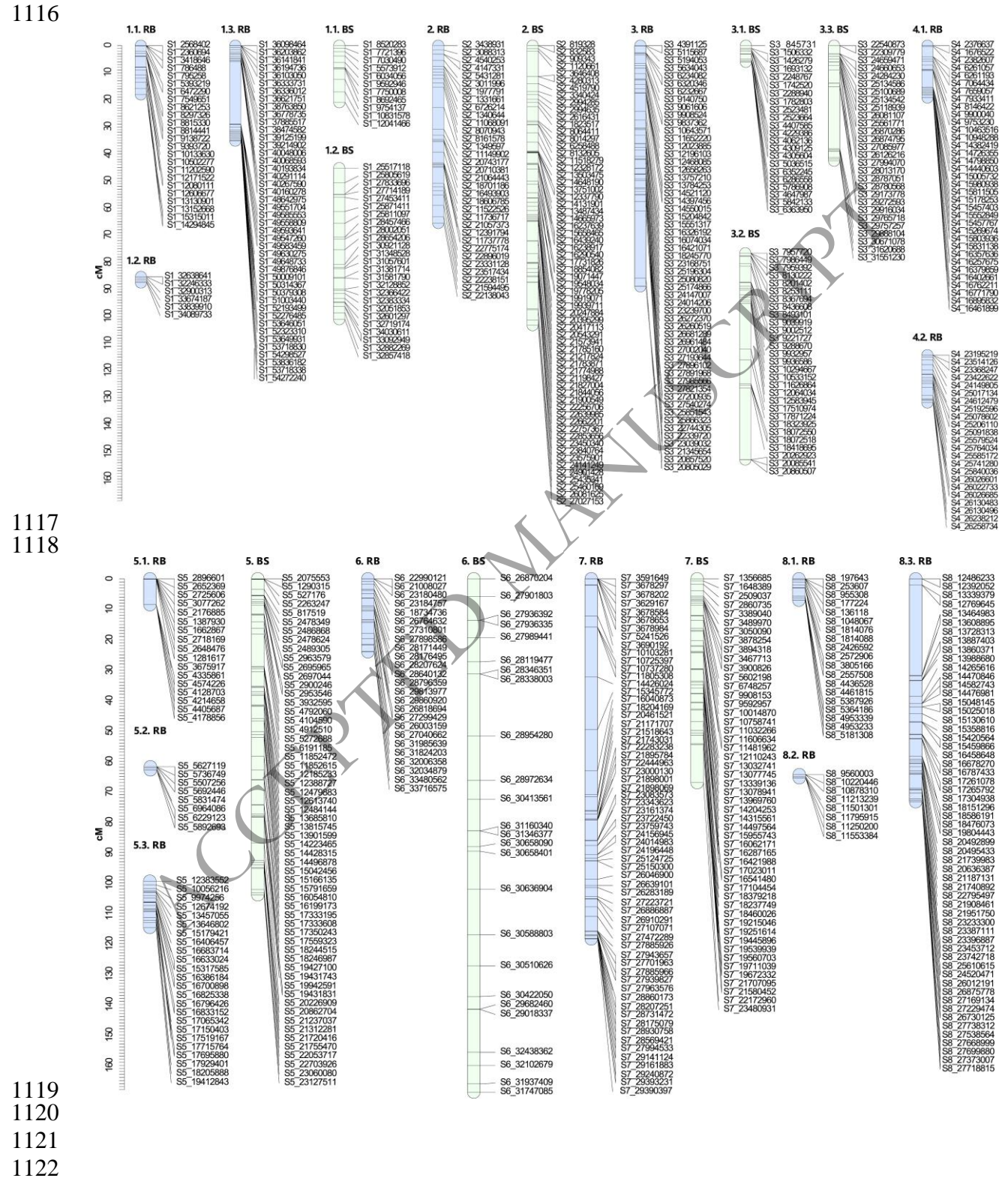


Figure 5. Genetic linkage maps for each genitor in the F_1 Japanese plum population 'Red Beaut' × 'Santa Rosa Precoz'. Markers positions are represented by black lines. The linkage groups of the female progenitor 'Red Beaut' (RB) are indicated in light blue, and those of the male progenitor 'Santa Rosa Precoz' (SRP) are indicated in green.

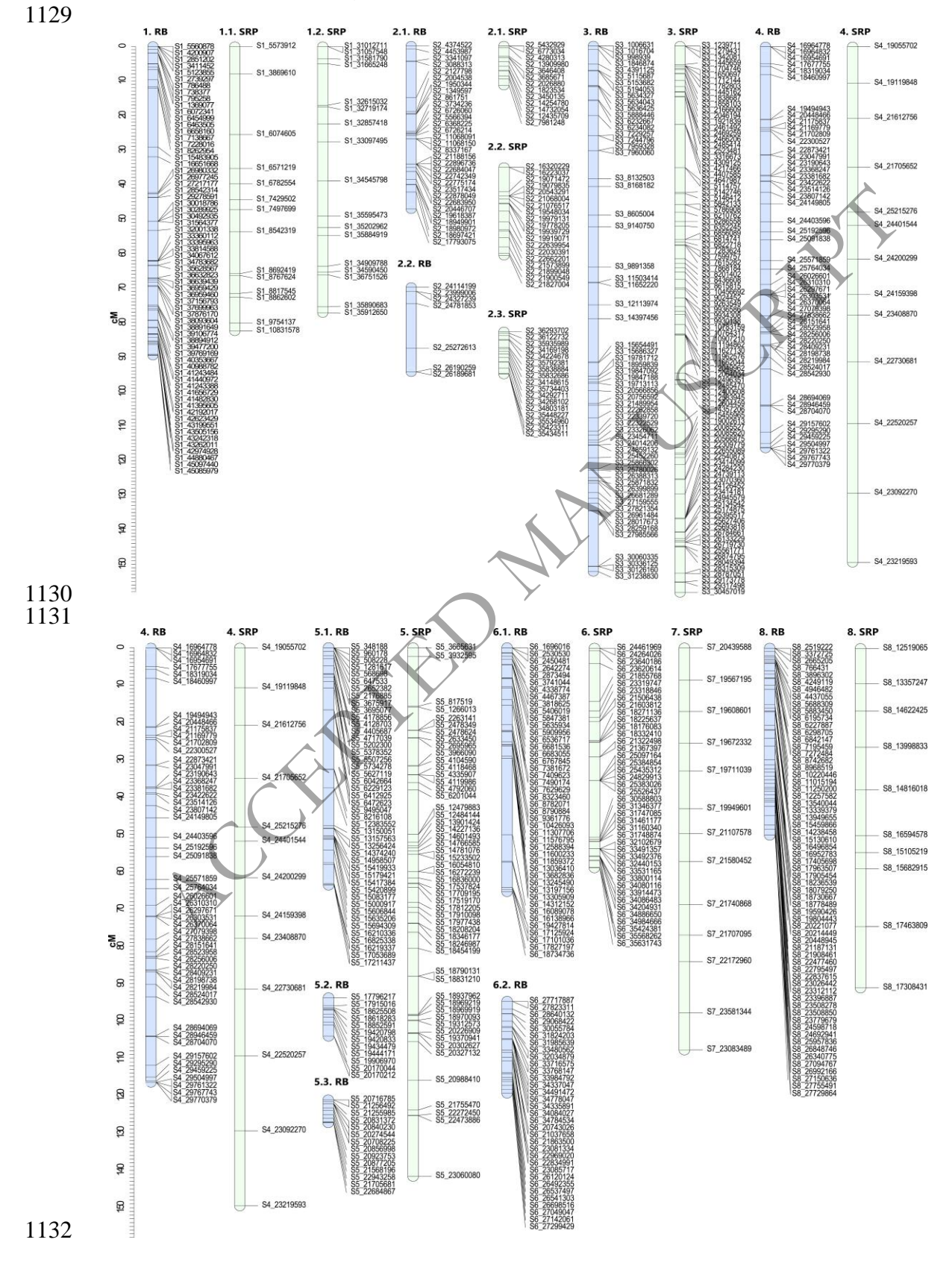


Figure 6. Consistent QTLs across the three years of phenotyping for phenological traits in the parents of the 'Black Splendor' (BS) × 'Pioneer' (PIO) population. The first number indicates the scaffold it represents, while the second number indicates the subgroup when multiple linkage groups are involved. The markers are listed on the right side of each LG, and the QTLs are depicted on the left side of their corresponding LGs. The representation of the QTLs includes a thick line indicating the most significant part of the QTL and a thin line indicating the entire significant interval (* p<0.01; *** p<0.005; *** p<0.001; **** p<0.0005; **** p<0.0001). The most significant markers of each QTL are shown in bold and in the color assigned to the trait.

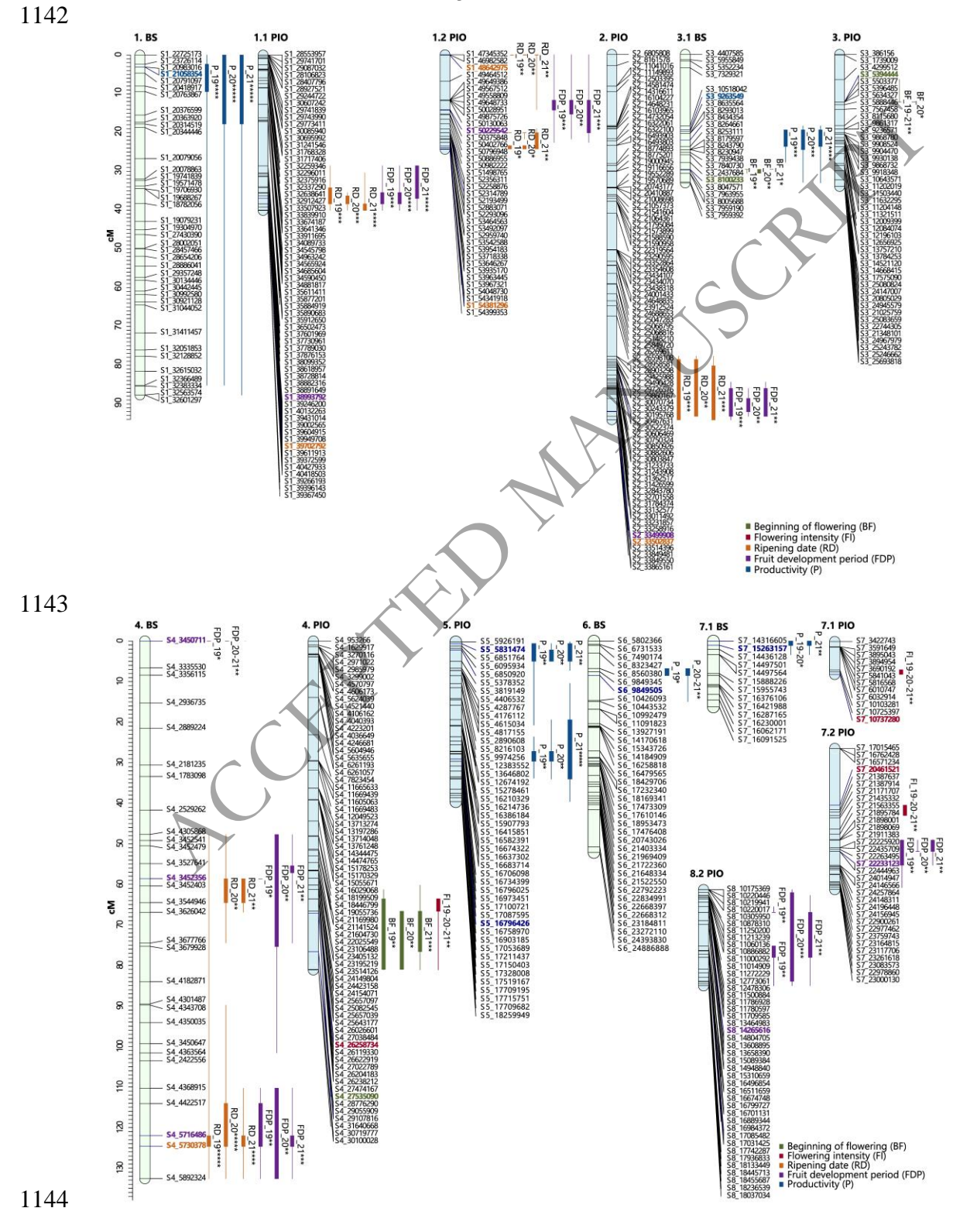


Figure 7. Consistent QTLs across the three years of phenotyping for phenological traits in the parents of the 'Red Beaut' (RB) × 'Black Splendor' (BS) population. The first number indicates the scaffold it represents, while the second number indicates the subgroup when multiple linkage groups are involved. The markers are listed on the right side of each LG, and the QTLs are depicted on the left side of their corresponding LGs. The representation of the QTLs includes a thick line indicating the most significant part of the QTL and a thin line indicating the entire significant interval (* p<0.01; ** p<0.005; *** p<0.001; **** p<0.0005; **** p<0.0001). The most significant markers of each QTL are shown in bold and in the color assigned to the trait.

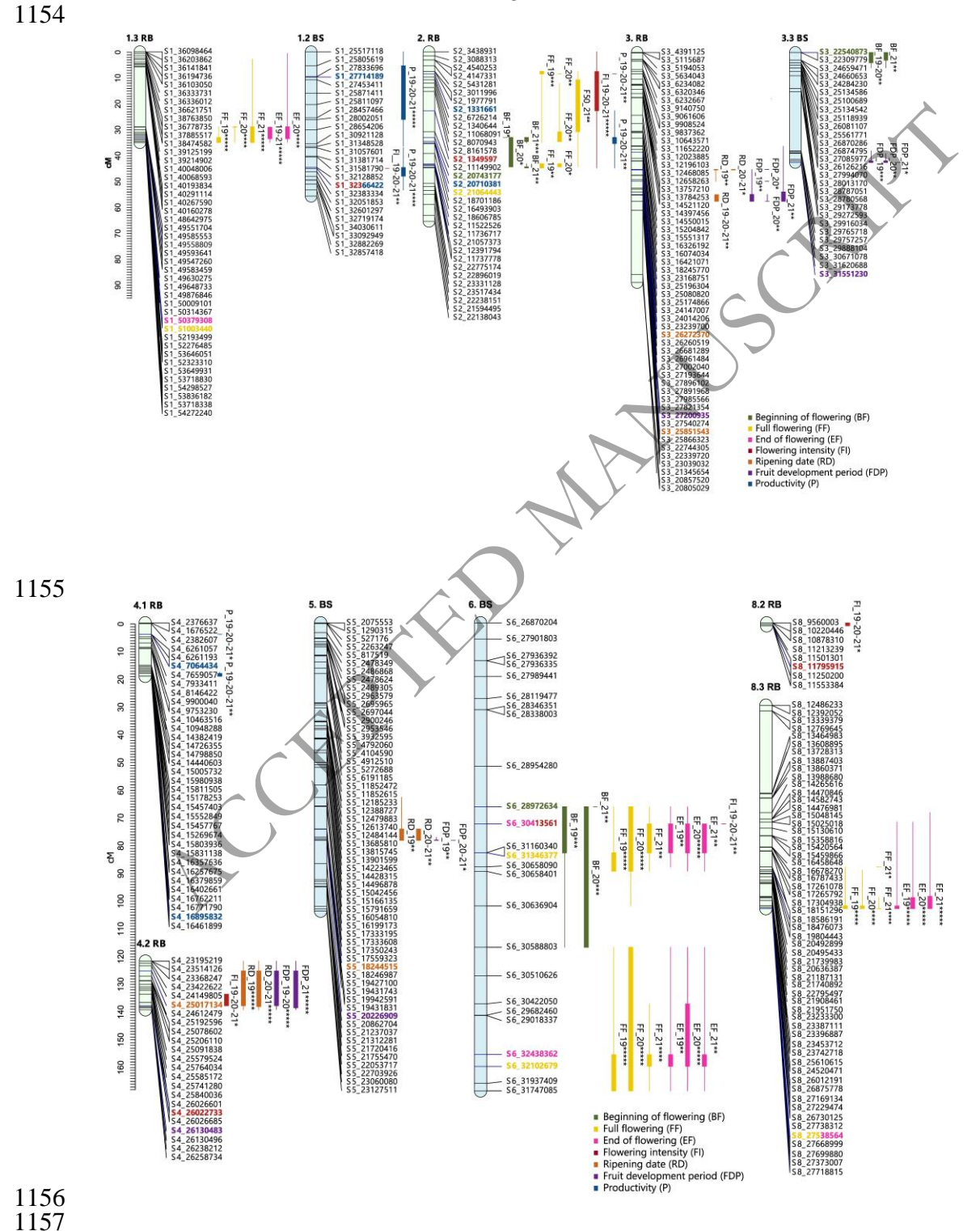
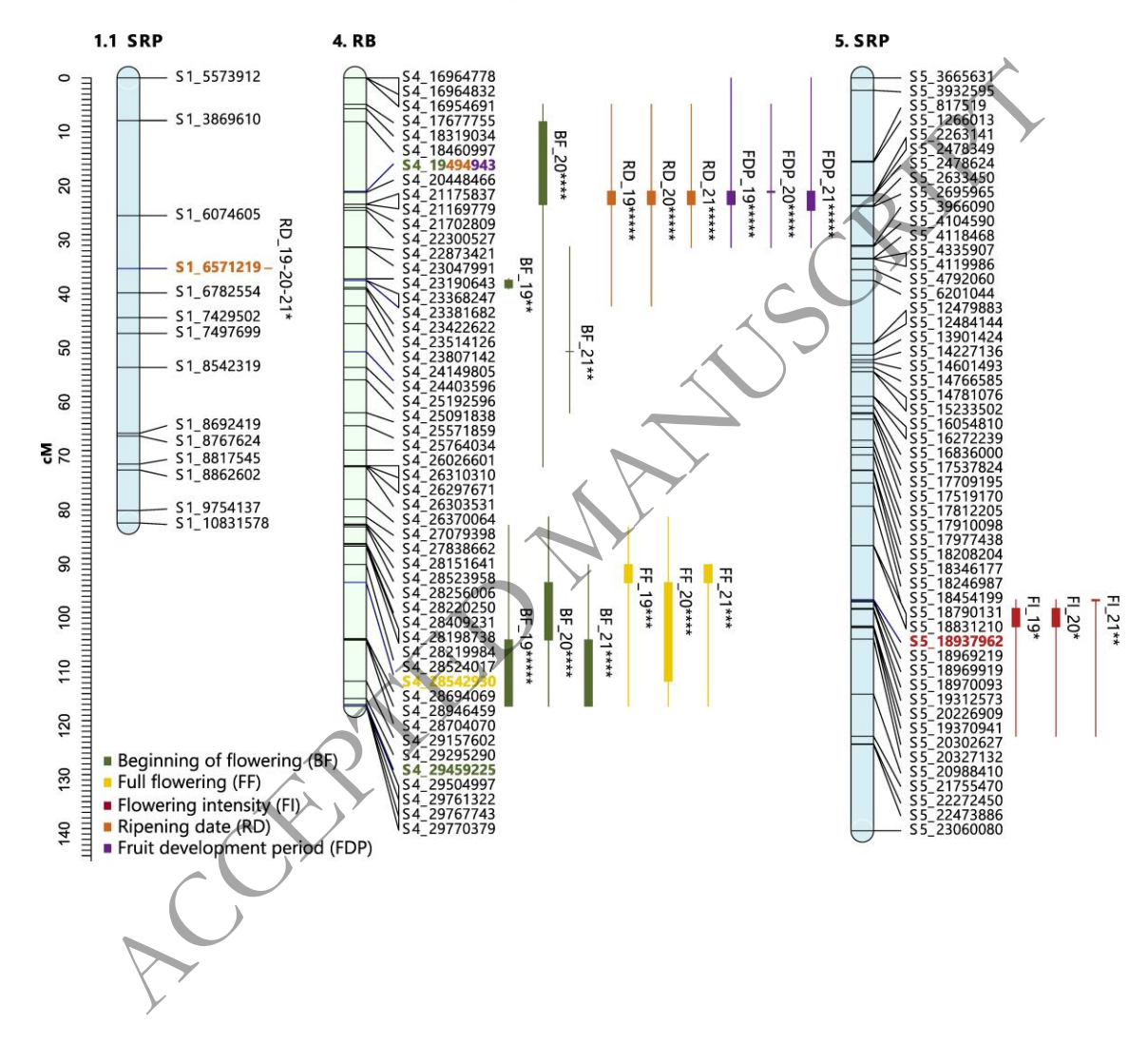


Figure 8. Consistent QTLs across the three years of phenotyping for phenological traits in the parents of the 'Red Beaut' (RB) × 'Santa Rosa Precoz' (SRP) population. The first number indicates the scaffold it represents, while the second number indicates the subgroup when multiple linkage groups are involved. The markers are listed on the right side of each LG, and the QTLs are depicted on the left side of their corresponding LGs. The representation of the QTLs includes a thick line indicating the most significant part of the QTL and a thin line indicating the entire significant interval (* p<0.01; ** p<0.005; *** p<0.001; *** p<0.005; **** p<0.0001). The most significant markers of each QTL are shown in bold and in the color assigned to the trait.



Supplementary Material

Figures

1177
1178 **Figure S1.** Frequency distribution of the 121 seedlings from 'Black Splendor' ×
1179 'Pioneer' F₁ Japanese plum progeny evaluated for different phenological traits
1180 including beginning of flowering (julian days, JD), full flowering (julian days), end

including beginning of flowering (julian days, JD), full flowering (julian days), end of flowering (julian days), flowering intensity (score from 0 to 3), ripening date (julian days), fruit development period (days) and productivity (score from 0 to 5) in the years 2019, 2020 and 2021. Arrows indicate the mean values of the

genitors, with BS for 'Black Splendor' and PIO for 'Pioneer'.

Figure S2. Frequency distribution of the 103 seedlings of 'Red Beaut' × 'Black Splendor' F₁ Japanese plum progeny evaluated for different phenological traits including beginning of flowering (julian days, JD), full flowering (julian days), end of flowering (julian days), flowering intensity (score from 0 to 3), ripening date (julian days), fruit development period (days) and productivity (score from 0 to 5) in the years 2019, 2020 and 2021. Arrows indicate the mean values of the genitors, with RB for 'Red Beaut' and BS for 'Black Splendor'.

Figure S3. Frequency distribution of the 103 seedlings of 'Red Beaut' × 'Santa Rosa Precoz' F₁ Japanese plum progeny evaluated for different phenological traits including beginning of flowering (julian days, JD), full flowering (julian days), end of flowering (julian days), flowering intensity (score from 0 to 3), ripening date (julian days), fruit development period (days) and productivity (score from 0 to 5) in the years 2019, 2020 and 2021. Arrows indicate the mean values of the genitors, with RB for 'Red Beaut' and SRP for 'Santa Rosa Precoz'.

Figure S4. A) Principal Component Analysis (PCA) biplot showing the seven phenological traits and the genotypes of each study population. 'Black Splendor' x 'Pioneer' (BSxPIO) progeny is represented by red circles, 'Red Beaut' x 'Black Splendor' (RBxBS) progeny by green triangles, and 'Red Beaut' x 'Santa Rosa Precoz' (RBxSRP) progeny by blue squares. The phenological traits represented are the beginning of flowering (BF), full flowering (FF), end of flowering (EF), flowering intensity (FI), ripening date (RD), fruit development period (FDP) and productivity (P). **B)** Scree plot displaying the percentage of explained variance for the first seven dimensions obtained from the analysis of phenological traits.

Figure \$5. Correlation matrix heat maps. Heat map of Spearman correlation between phenological traits during the three years of study in the populations 'Black Splendor' x 'Pioneer' (A), 'Red Beaut' x 'Black Splendor' (B), and 'Red Beaut' x 'Santa Rosa Precoz' (C). The phenological traits represented are the beginning of flowering (BF), full flowering (FF), end of flowering (EF), flowering intensity (FI), ripening date (RD), fruit development period (FDP) and productivity (P). Within each module, the p-value significance level of the correlation is indicated by asterisks (*), where p<0.05 is represented as *; p<0.01 as ** and p<0.001 as ***.

- 1223 Figure S6. Alelic effect of the SNP marker 'S6_32102679' from the 'Black Splendor' (BS) parent of the RB×BS population. Each box plot represents the 1224 1225 distribution in Julian days (JD) for full flowering (FF), differentiating between the genotypes "CC" and "CT" of the SNP marker 'S6 32102679'. The p-value derived 1226 1227 from the Kruskal-Wallis test is presented to compare the median FF dates 1228 between the different phenotypes across the three years of study.
- Figure S7. Alelic effect of the SNP marker 'S3 22540873' from the 'Black 1230 Splendor' (BS) parent of the RB×BS population. Each box plot represents the 1231 1232 distribution in Julian days (JD) for beginning of flowering (BF), differentiating between the genotypes "AA" and "AG" of the SNP marker 'S3 22540873'. The 1233 1234 p-value derived from the Kruskal-Wallis test is presented to compare the median 1235 BF dates between the different phenotypes across the three years of study.
 - Figure S8. Alelic effect of the SNP marker 'S2 1349597' from the 'Red Beaut' (RB) parent of the RB×BS population. Each box plot represents the distribution for flowering intensity (FI), differentiating between the genotypes "TT" and "CT" of the SNP marker 'S2 1349597'. The p-value derived from the Kruskal-Wallis test is presented to compare the median flowering intensity between the different phenotypes across the three years of study
 - Figure S9. Alelic effect of the SNP marker 'S4 19494943' from the 'Red Beaut' (RB) parent of the 'RB×SRP' population. Each box plot represents the distribution in Julian days (JD) for ripening date (RD) and in days (D) for the fruit development period (FDP), differentiating between the genotypes "AA" and "AT" of the SNP marker 'S4 19494943'. The p-value derived from the Kruskal-Wallis test is presented to compare the median distribution of both traits between the different phenotypes across the three years of study.

TablesS

1229

1236 1237

1238

1239

1240

1241

1242

1243

1244

1245

1246 1247

1248 1249

1250

1251 1252 1253

1254

- **Table S1.** Parental genotypes information, including origin and main agronomic 1255 characteristics (self-compatibility, flowering and ripening time and skin and flesh 1256 1257 colour).
- Table \$2. Whole Genome Sequencing (WGS) of the parental lines 'Santa Rosa 1259 Precoz'\(SRP), 'Pioneer' (PIO), 'Red Beaut' (RB), and 'Black Splendor' (BS). The 1260 raw data generated by the sequencer, as well as the raw and retained reads, are 1261 1262 shown. The percentage of retained reads is indicated in parentheses.
- 1263 **Table S3.** Quality assessment metrics of the whole genome assembly obtained 1264 with MaSuRCA for the parental lines 'Santa Rosa Precoz' (SRP), 'Pioneer' (PIO), 'Red Beaut' (RB), and 'Black Splendor' (BS). Metrics include: number of 1265 assembled contigs (≥ 0 bp, 1000 bp, 5000 bp, etc.); total length of assembled 1266 1267 sequences by contig size; GC content; N50 and N75; lengths of the shortest contigs covering 50% and 75% of the total assembly length; L50 and L75: number 1268 1269 of contigs needed to reach 50% and 75% of the total assembly length; number of
- 1270 ambiguous sequences (N's) per 100 kbp of assembled DNA.

- 1271 **Table S4**. Alignment of reads with the MaSuRCA whole-genome assemblies of
- 1272 'Santa Rosa Precoz' (SRP), 'Pioneer' (PIO), 'Red Beaut' (RB), and 'Black
- 1273 Splendor' (BS). Exact alignment rates are shown in parentheses.
- 1274 **Table S5.** BUSCO quality analysis of the whole-genome assemblies of the
- parental lines 'Santa Rosa Precoz' (SRP), 'Pioneer' (PIO), 'Red Beaut' (RB),
- 1276 and 'Black Splendor' (BS).
- 1277 **Table S6.** Deletions, insertions, and SNPs observed in the whole-genome
- assemblies of 'Santa Rosa Precoz' (SRP), 'Pioneer' (PIO), 'Red Beaut' (RB), and
- 1279 'Black Splendor' (BS).
- 1280 **Table S7.** Distribution of transitions and transversions in genetic variants for the
- whole genomes of 'Santa Rosa Precoz' (SRP), 'Pioneer' (PIO), 'Red Beaut' (RB),
- and 'Black Splendor' (BS), with the number and percentage of allelic sites in
- 1283 parentheses.
- 1284 **Table S8.** Number of SNPs at each stage of genetic map construction.
- 1285 **Table S9**. Summary of descriptive statistics and Kolmogorov-Simornov test of the
- evaluated traits in the three populations 'Black Splendor' x 'Pioneer' (BSxPIO),
- 1287 'Red Beaut' x 'Black Splendor' (RBxBS) and 'Red Beaut' x 'Santa Rosa Precoz'
- 1288 (RBxSRP) F₁ progenies during the three years of study.
- 1289 **Table S10**. Kruskal–Wallis analysis for independent samples for the year factor
- was performed on the evaluated traits that exhibit a non-parametric distribution
- in the populations 'Black Splendor' × 'Pioneer' (BS×PIO), 'Red Beaut' × 'Black
- 1292 Splendor' (RBxBS), and 'Red Beaut' x Santa Rosa Precoz' (RBxSRP). Bolded
- values indicate significant differences in the distribution of the traits.
- 1294 **Table S11.** Bonferroni test for multiple comparisons of the year factor on traits
- and populations with significant differences between years in the populations
- 1296 'Black Splendor' × 'Pioneer' (BS×PIO), 'Red Beaut' × 'Black Splendor' (RB×BS),
- and 'Red Beaut' x 'Santa Rosa Precoz' (RBxSRP). CE: Contrast statistic; DES.
- 1298 EC: Deviation of the contrast statistic; Sig.: Significance. Bolded values indicate
- that there are significant differences in that comparison.
- 1300 **Table S12.** Spearman correlation coefficient between the years 2019, 2020 and
- 1301 2021 for the phenological trait assessed in the populations 'Black Splendor' ×
- 1302 'Pioneer' (BS×PIO), 'Red Beauty' × 'Black Splendor' (RB×BS) and 'Red Beauty'
- 1303 × 'Santa Rosa Precoz' (RB×SRP). The p-value significance level of the
- correlation is indicated by asterisks (*), where p<0.05 is represented as *; p<0.01
- 1305 as ** and p<0.001 as ***.

1307

1308

- 1310 **Table S13.** Summary of SNP marker mapping in the genetic linkage maps
- obtained for the parental lines 'Black Splendor' (BS), 'Pioneer' (PIO), 'Red Beaut'
- 1312 (RB), and 'Santa Rosa Precoz' (SRP) from the three studied populations: 'Black
- 1313 Splendor' × 'Pioneer' (BS×PIO), 'Red Beaut' × 'Black Splendor' (RB×BS), and
- 1314 'Red Beaut' × 'Santa Rosa Precoz' (RB×SRP).

- 1316 **Table S14.** Description of the phenology QTLs identified for each parent of the
- 1317 'Black Splendor' (BS) × 'Pioneer' (PIO) population through Kruskal-Wallis (KW).
- The level of significance is indicated by asterisks (*), where p<0.01 is represented
- as *; p<0.005 as **; p<0.001 as ***; p<0.0005 as ****; and p<0.0001 as ****. LG:
- linkage group; K: KW test statistical value; C: QTL consistency across the study
- 1321 years.
- 1322 **Table S15.** Description of the phenology QTLs identified for each parent of the
- 1323 'Red Beaut' (RB) × 'Black Splendor' (BS) population through Kruskal-Wallis (KW).
- The level of significance is indicated by asterisks (*), where p<0.01 is represented
- as *; p<0.005 as **; p<0.001 as ***; p<0.0005 as ****; and p<0.0001 as ****. LG:
- linkage group; K: KW test statistical value; C: QTL consistency across the study
- 1327 years.
- 1328 **Table S16.** Description of the phenology QTLs identified for each parent of the
- 1329 'Red Beaut' (RB) × 'Santa Rosa Precoz' (SRP) population through Kruskal-Wallis
- 1330 (KW). The level of significance is indicated by asterisks (*), where p<0.01 is
- represented as *; p<0.005 as **; p<0.001 as ***; p<0.0005 as ****; and p<0.0001
- as ****. LG: linkage group; K: KW test statistical value; C: QTL consistency across
- the study years.
- 1334 **Table S17.** Parental genotypes of the 'Black Splendor' × 'Pioneer' population for
- the most significant SNP markers of each QTL associated with phenological traits
- and their allelic effects. The SNP is presented in bold. Allelic effects are significant
- at a minimum of p<0.05 over the three-year study period according to the
- 1338 Kruskal–Wallis test
- 1339 **Table S18.** Parental genotypes of the 'Red Beaut' × 'Black Splendor' population
- for the most significant SNP markers of each QTL associated with phenological
- traits and their allelic effects. The SNP is presented in bold. Allelic effects are
- significant at a minimum of p<0.05 over the three-year study period according to
- the Kruskal–Wallis test.
- 1344 **Table S19.** Parental genotypes of the 'Red Beaut' × 'Santa Rosa Precoz'
- population for the most significant SNP markers of each QTL associated with
- phenological traits and their allelic effects. The SNP is presented in bold. Allelic
- effects are significant at a minimum of p<0.05 over the three-year study period
- 1348 according to the Kruskal–Wallis test.

1349

- 1350 **Table S20.** Overview of the characteristics of existing Japanese plum genetic
- maps, including those generated in the present study.

Table S21. The predicted effects for each significant SNP associated with stable QTLs and candidate genes identified. In addition, each studied trait is represented by columns that have been colored for each significant effect (the allelic effect was added, colours without letter means no studied effects) and SNP